Experimental Comparison of Calcium Sulfate ($CaSO_4$) Scale Deposition on Coated Carbon Steel and Titanium Surfaces

By

DHAWI ABDULRAHMAN AL-OTAIBI

A Thesis Presented to the

DEANSHIP OF GRADUATE STUDIES

In Partial Fulfillment of the Requirement

for the Degree of

MASTER OF SCIENCE
In

MECHANICAL ENGINEERING

KING FAHD UNIVERSITY
OF PETROLEUM & MINERALS

DHAHRAN, SAUDI ARABIA

November, 2008

KING FAHD UNIVERSITY OF PETROLEUM & MINERALS
DHAHRAN 31261, SAUDI ARABIA

DEANSHIP OF GRADUATE STUDIES

This thesis, written by Dhawi AbdulRahman Al-Otaibi under the direction of his thesis advisor, and approved by his thesis committee, has been presented to and accepted by the Dean of Graduate Studies, in partial fulfillment of the requirements for the degree of **MASTER OF SCIENCE IN MECHANICAL ENGINEERING**

Thesis Committee

_____
Dr. Luai M. Al-Hadhrami (Advisor)

_____
Dr. Mohammed A. Antar (Member)

_____
Dr. Salem A. Al-Dini (Member)

_____
Dr. Amro M. Al-Qutub
Department Chairman

_____
Dr. Salam A. Zummo
Dean of Graduate Studies

_____
Date

Dedicated to

My beloved parents and family, whose sacrifices enabled me to reach this stage

Acknowledgments

In the name of ALLAH, the most merciful and beneficent.

"Verily, my prayer, my sacrifices, my living, and my dying are for ALLAH, the Lord of Alamin (mankind, jinn and all that exists)".

"He has no partner. And of this I have been commanded, and I am the first of Muslims."

All praise to almighty ALLAH Who gave me the patience and perseverance to carry out this research successfully.

Acknowledgment is due to King Fahd University of Petroleum and Minerals (KFUPM)/ Research Institute (RI) for providing full support to this work.

I deeply appreciate my thesis committee Chairman Dr. Luai M. Al-Hadhrami, and also Dr. Mohammed A. Antar and Dr. Salem A. Al-Dini, for their constant help, guidance and attention throughout this research. My many questions to them always generated a cheerful response. Thanks to Dr. Al-Hadhrami, Dr. Al-Dini and Dr. Antar for introducing me to a new dimension in the world of heat transfer.

Thanks are due also to Mr. Abdul Quddus from CER/RI, whose continued assistance and guidance made the experimental task successful. I greatly appreciate his pivotal role in achieving my objectives related to the experimental work.

Last but not least, thanks are due to my family members and friends for their unlimited support and understanding, throughout my academic career. Special thanks to my parents and my wife for their patience and encouragement throughout this research.

Table of Contents

List of Figures

List of Tables

ملخص الرسالة

إسم الباحث : ضاوي عبدالرحمن العتيبـــي

عنوان الرسالة : مقارنة عملية في ترسب كبريتات الكالسيوم على سطح معدن الفولاذ المطلي و التيتينيوم

التخصص الرئيسي : الهندسة الميكانيكية

تاريخ الدرجة : نوفمبر 2008 م

ترسب أملاح كبريتات الكالسيوم يقلل معامل الانتقال الحراري في معدات الانتقال الحراري الذي بدوره يؤثر على فعالية معدات التبادل الحراري وبتالي يؤثر على إنتاجية المصانع البتروكيميائية و البترولية. إن البحث الحالي يحتوي على تجارب عملية وتحليل بياني لنتائج متعلقه بترسب أملاح كبريتات الكالسيوم على سطح معدن الحديد المطلي بمادة السكافن (Sakaphen) و التيتينيوم باستخدام جهاز الألكترود الأسطواني الدوار. بالإضافة الى ذلك تم تصويروفحص تشكّل و توزيع ترسبات قشور كبريتات الكالسيوم على سطح معدن التيتينيوم باستخدام الفاحص المجهري الإلكتروني. في هذه الدراسة سرعة جهاز الألكترود الأسطواني الدوار رفعت من 100 إلى 2000 دورة في الدقيقة لدراسة ترسب أملاح كبريتات الكالسيوم على كلا المعدنين. بناء على نتائج التجارب يتضح التالي, ترسب أملاح كبريتات الكالسيوم شبه ثابت على سطح معدن الحديد المطلي بينما تزداد كمية الأملاح مع زيادة سرعة الدوران على سطح معدن التيتينيوم. كذلك تم دراسة مجموعة مما تم نشره في السابق بخصوص هذا الموضوع.

Abstract

Name: **Dhawi AbdulRahman Al-Otaibi**

Title: **Experimental Comparison of Calcium Sulfate ($CaSO_4$) Scale Deposition on Coated Carbon Steel and Titanium Surfaces**

Major Field: **Mechanical Engineering**

Date of Degree: **November, 2008**

Calcium Sulfate ($CaSO_4$) deposit reduces heat exchange in heat transfer equipment which adversely affects the equipment performance and plant production. This experimental study was conducted by using the Rotating Cylinder Electrode (RCE) equipment available in the university's Center for Engineering Research (CER/RI) to study and compare the effect of solution hydrodynamics on Calcium Sulfate ($CaSO_4$) scale deposition on coated carbon steel and titanium surfaces. In addition, the Scanning Electron Microscopic was used to examine the morphology and distribution of Calcium Sulfate ($CaSO_4$) crystals deposited on titanium metal surfaces. In this study, the rotational speed was varied from 100 to 2000 RPM to study the behavior of Calcium Sulfate ($CaSO_4$) accumulation on both materials. Based on the experimental results, Calcium Sulfate ($CaSO_4$) scale obtained in the present study was almost constant on coated carbon steel in which the rate of scale deposition is equal to the rate of scale removal. However, the deposition of Calcium Sulfate ($CaSO_4$) observed on titanium material was increased as the speed increased.

CHAPTER 1

INTRODUCTION

Fouling formation and under-deposit corrosion caused by scale deposit are two of the challenging problems encountered in the petroleum and petrochemical industries. Heat transfer equipment such as heat exchangers, process fired heaters and boilers are used extensively in several industrial applications such as power generation, refineries, petrochemicals and desalination plants to recover heat from hot fluid streams. Deposit accumulation inside or outside the tube reduces the capability of heat transfer equipment to exchange heat. It degrades their efficiency which increases the operating cost and sometimes causes unplanned plant shutdowns and production losses. The major factor behind the efficiency decrease is the scale deposition accumulation and the build-up of unwanted materials on the heat transfer surface, which is well known as "Fouling or Scaling". The scale deposition has very low thermal conductivity, which imposes further resistance in addition to those present in any typical design of the exchanger. Moreover, the scale build-up reduces the flow area, which results in an additional pressure drop through the heat exchanger and the whole plant's hydraulic system, thus increasing the energy consumption.

To mitigate corrosion and fouling, expensive corrosion-resistant alloys are used as construction materials for shell and tube heat exchangers. The use of titanium tubes in heat exchangers is a common practice nowadays, which has resulted in an exceptional increase of service life in many refinery heat exchangers. The copper

based alloys such as Copper-Nickel (Cu-Ni) are the most effective tube material used in desalination plants. However, due to seawater corrosion, the leak developed may cause serious problems. Titanium has been used either as original equipment or for retubing. Capital and maintenance costs of heat exchangers can be reduced considerably if coated carbon steel tubes are used instead of expensive high alloy materials such as Copper-Nickel or Titanium. Carbon steel tubes are coated with a low-cost and thermally conductive coating that provides corrosion resistance as well. In aggressive environments, heat exchangers' capital and maintenance costs are high, due to the use of expensive corrosion resistance materials [1]. Heat exchanger fouling or deposition accumulation in general is a major economic problem accounting for 0.25 % of the total gross domestic product (GDP) in highly industrialized countries [2].

A methodology was developed earlier in the laboratory by the use of a Rotating Cylinder Electrode (RCE) to study scale build-up on different metal surfaces. RCE is used to simulate conventional pipe flow [3]. This technique has some advantages over conventional flow loop test methods, due to the ease of creating turbulent flow conditions and the simplicity in handling and operating the whole test equipment. Although the boundary conditions are different in conventional flow loop (V = 0 at pipe wall, V= maximum at middle) and RCE ($\omega = 0$ at the cell wall, ω = maximum at the sample wall), scientists successfully modeled the velocity-affected corrosion mechanism. This was accomplished by equating the wall shear stresses in RCE to the pipe geometry under similar hydrodynamic conditions, for example turbulence, which resulted in identical mass transfer coefficients of both geometries [3]. In the present experiment, the effect of solution hydrodynamics is studied at different rotational

speeds (RPM) to obtain and compare Calcium Sulfate ($CaSO_4$) scale deposition on coated carbon steel and titanium surfaces. The economic impact of these two metals is also studied to show the difference between them in terms of scale elimination and equipment capital cost reduction.

1.1 Literature Review

Fouling or deposit accumulation is a severe problem in heat transfer surfaces. Fouling results from the accumulation of suspended particles in liquid or gas streams onto heat transfer surfaces [5]. Particle accumulation due to gravity is referred to as sedimentation. The suspended particles may include ambient pollutants such as sand, iron, and microbial organisms in cooling water.

Precipitation fouling is the deposition of a solid layer on heat transfer surfaces. It occurs when the process conditions lead to supersaturation of the dissolved inorganic salts on the heat transfer surfaces. These conditions which lead to supersaturation involve evaporation beyond solubility limits, cooling/heating beyond solubility limits, or mixing of the process stream. The industrial systems and operations in which the problem of precipitation fouling is significant are: Saline Desalination Plants, Geothermal Brine Systems, Cooling Water Systems, Steam Generation Systems and Potable Water Supply Systems. Some dissolved species show inverse solubility versus temperature behavior. In this case, the substance tends to precipitate on a heated rather than a cooling surface, as seen in cooling water applications. Calcium Sulfate ($CaSO_4$), which is our main focus in this research, is one of the salts that exhibit this behavior. The driving force for crystallization is the chemical potential

difference between the substances in the solution and the deposit formed on the metal surface [5].

The effect of supersaturation, pH, Reynold number and concentration of ions in the brine solution on the formation of silica scale in heat-exchanger tubes were discussed, and also a silica deposition model was proposed by Neusen et al. [6].

Chemical reaction fouling includes deposits that are formed as a result of chemical reactions within the process fluid. Although a heat exchanger surface does not act as a reactant, it sometime behaves as a catalyst [7]. This type of fouling occurs commonly in chemical process industries, refineries and the dairy process.

Hopkinson et al. [8] investigated the use of titanium tubes in petroleum refining heat exchangers. Their investigation was conducted on 40 operating heat exchangers. Their results revealed that the use of titanium tubes for heat exchangers gave an exceptional increase in the service life of many refinery heat exchangers. The service life of the exchangers and the plant production were improved by the use of titanium tubes.

Scholl [9] reported that the capital costs of a typical heat exchanger can be reduced to 67% if polymer-coated carbon steel tubes, tubesheets, and headers are used in place of titanium tubes and titanium-clad plates. Scale deposit on coated surfaces is reduced tremendously, compared with non-coated parts. Scale mitigation on heat transfer equipment improves the equipment performance and reduces the plant's production losses.

Gawlik et al. [1] tested different types of polymer-based coatings. They coated carbon steel tubes in four heat exchangers to protect these from corrosion and to mitigate the strong adherence of scale and fouling formation. Laboratory and field tests of coated tubes showed that the deposit bonded to the coated tubes was weaker than that on expensive tubing materials such as stainless steel and titanium. The coated tubes can be cleaned easily by using conventional hydroblasting methods without damage to the coating. However, cleaning non-coating tubes such as Titanium is a difficult process since scale adheres firmly to the metal surfaces.

Neville et al. [10] studied the nucleation and growth of Calcium Carbonate ($CaCO_3$) scale on a Stainless Steel 316L metal surface in a supersaturated solution by using a rotating disc electrode (RDE). Their method was based on the correlation between the diffusional characteristic of oxygen at a metal surface and the change in the rate of oxygen reduction once nucleation and growth of the $CaCO_3$ starts. They found that the technique helped in the assessment of the scale buildup on metal surfaces, and their results were supported with the image analysis, which showed similarity especially at high surface coverage.

Quddus and Allam [11] studied the deposition of $BaSO_4$ scale on stainless steel-316 specimens by using the Rotating Cylinder Electrode (RCE) apparatus. They noticed that, as the Reynolds number increased, a high rate of scale deposition on the electrode surface took place. This showed that the process was diffusion-controlled. The morphology examination of the scale by Scanning Electron Microscopy (SEM) revealed that the $BaSO_4$ crystals were dense and uniformly distributed over the metal surface.

Quddus [12] investigated Calcium Sulfate ($CaSO_4$) deposition on stainless steel-316 specimen by using RCE. He found that Calcium Sulfate ($CaSO_4$) scale deposition on a metal surface is influenced by the Reynolds number. This means that, as rotational speed increases, the scale deposition on the metal surface also increases. This is in agreement with what had been noticed in the case of $BaSO_4$. However, examining the scale crystals by SEM revealed that Calcium Sulfate ($CaSO_4$) crystals initially grow perpendicular to the substrate and then branch out randomly in all directions, which was considered a typical characteristic of the Calcium Sulfate ($CaSO_4$) scale. However, crystal structures of the $BaSO_4$ scale did not experience this pattern.

Neville and Morizot [13,14] studied scale build-up on steel by using Rotating Disc Electrode apparatus under application of cathodic protection in three different solutions. They noticed that, in the solution containing both Magnesium (Mg) and Calcium (Ca), a densely packed fine crystal basal layer (initial thin layer) rich in Magnesium (Mg) was formed, which contained needles identified as Aragonite (a form of $CaCO_3$ scale). In a solution that did not contain Calcium (Ca), they found that a similar deposition to the previous one occurred, except that the needles crystals were absent. In the solution that had no Magnesium (Mg) ions, the growth of $CaCO_3$ was promoted, and the scaling crystal was characteristic of Calcite (another form of $CaCO_3$ scale). Those results showed that the existence of Magnesium (Mg) ions in the solution encouraged the formation of the Aragonite form of $CaCO_3$ and prevented the Calcite structure.

Chen et al. [15] studied the $CaCo_3$ scale formation and adhesion on Stainless Steel type-316 metal surface by using an electrochemical-based technique. This technique monitors the scale coverage by measuring the oxygen reduction on the specimen under potentiostatic control. They found that the precipitation in the bulk solution is affected by the concentration of ions in the solution. For bulk precipitation, a higher concentration revealed a shorter induction period (the time between supersaturation creation and the first observable change in the solution's physical properties).

Gabe et al. [16] reviewed the application of the rotating cylinder electrode (RCE) in electrochemistry during the period from 1982 to 1995. Different geometries (namely rotating cylinder electrode, rotating cone electrode, rotating hemispherical electrode, rotating wire electrode and rotating disk electrode) were covered in their review. They found that RCE was generally accepted and widely used. Also, the mass transported to the electrode could be altered and controlled by some factors such as surface roughness.

Branch and Muller [17] studied the influence of scaling on the performance of shell and tube heat exchangers. They modeled the fouling mechanism in both types of heat exchanger. Four configurations were examined, in which they had different relative positions of the inlet nozzles. All these four arrangements showed a clear dependence of scaling on the temperature distribution. They found that scaling could be predicted, even with a negative temperature difference between the heat transfer surface and the working fluid. In addition, they noticed that, when scaling took place in all four configurations, there were no major differences in the temperature distribution among the different patterns.

Fahiminia et al. [18] studied experimentally the effect of temperature and velocity on the initial scaling rate of the inverse solubility salt $CaCO_3$ under sensible heating conditions. The bulk inlet temperature was 55 ˚C while the clean surface temperatures varied from 80 to 101 ˚C, and the Reynolds numbers varied from 7000 to 21000. They found that, as the temperature and velocity of the bulk increase, the delay time (the period of time elapsed between the occurrence of supersaturation and the first detection of fouling deposition on the metal surface) decreases for velocities below 0.5 m/s. However, the delay time remains approximately constant at higher velocities.

Sheikhholeslami and Ng [19] studied the fouling of heat exchangers under co-precipitation of inorganic salts. They investigated the co-precipitation process of $CaCO_3$ and $CaSO_4$ when sulfate SO^{-}_4 was the dominant anion. They observed no induction period associated with the co-precipitation process, and scaling initiated almost immediately. Also, they noticed that the precipitation was fine and had a loosely adhering layer for pure $CaSO_4$. They concluded that, as the concentration of $CaCO_3$ increased, it tended to be tenacious and more strongly adherent. When the solution contained only pure $CaSO_4$, the precipitate had long needle-shaped crystals floating in the solution.

Behbahani et al. [20] investigated tube-side fouling of a heat exchanger exposed to a solution of Calcium Sulfate ($CaSO_4$) mixed with high concentration phosphoric acid (H_3PO_4). His study focused on the different solubility of Calcium Sulfate ($CaSO_4$) in acid solution (H_3PO_4). His results showed that, for the range of solution velocity of 1.3 – 1.8 m/s, the solubility had an inverse linear relationship with the fouling resistance. He also found that, as the tube surface temperature increased, the fouling

resistance also increased. The change in the fouling resistances was temperature-sensitive.

Helalizadeh et al. [21] studied experimentally the effects of various operating parameters, such as solution composition and hydrodynamic of the system, on the crystallization fouling of Calcium Sulfate ($CaSO_4$) and Calcium Carbonate ($CaCO_3$) mixtures under convective heat transfer and sub-cooled flow boiling conditions. They found that the resultant scale depended on the ionic concentration of both salts. Fouling crystallization during the formation of bubbles on the heat transfer surface was high, and the salts concentration below the bubbles increased significantly, which resulted in the formation of a scale deposit on the heat transfer surfaces.

Yang et al. [22] investigated the induction period of Calcium Carbonate ($CaCO_3$) fouling on heated Self-Assembled Monolayer (SAM). They studied the morphologies of Calcium Carbonate ($CaCO_3$) in the presence and absence of the antifouling polyacrylic acid (PAA). They found that, at constant initial surface temperature and similar experimental conditions, SAMs material experienced an induction period of one hour after the start of the test, while there was no induction period for copper. As the velocity increased, more foulant ions diffused to the surface which minimized the induction period. When both fluid velocity and initial surface temperature were taken into consideration, the initial surface temperature influenced the induction period occurrence more than fluid velocity did.

Klaren et al. [23] proposed a novel design for shell and tube heat exchangers, which employed a self-cleaning principle. A clean intermediate shell-side fluid, flowing in the shell of both exchangers, transfers heat between two parallel bundles. As a result,

the zero-fouling self-cleaning heat exchanger required only one-third of the heat transfer surface area that was needed by the conventional type. A longer period of operation can be achieved between inspections or cleanings. Also, one important factor is that the pumping power required for a zero-fouling self-cleaning heat exchanger was less than that for a conventional heat exchanger.

Liu et al. [24] examined the relationship of corrosion in a rotating disk system and that in the turbulent pipe flow system. A closed-form mathematical model was developed, and it was in close agreement with the experimental results of other researchers. Eventually, the pipe corrosion was predicted by using experimental data obtained with the help of a rotating disk electrode.

Efrid et al. [25] quantified the relationship of laboratory fluid flow data corrosion test techniques to field applications. They used jet impingement and RCE techniques, which were compared directly to simultaneous pipe-flow experiments. They found that the RCE technique provided a stable and reproducible turbulent flow with relatively small volumes of test fluid, but RCE cannot be used for high pressure or high temperature applications or even for gas and gas/liquid systems. They found that the basic equation for the effect of wall-shear stress on carbon steel, which relates the rate of corrosion to wall shear stress, is good enough for corrosion prediction.

Silverman [26] reviewed the relationship between mass transfer coefficient, fluid velocity, shear stress and fluid properties in four geometries. He showed how corrosion in different geometries may be related in terms of the best information on shear stress, friction factor and Sherwood number. This was performed to decide which RCE geometry might be used for testing purposes. He concluded that

modeling the velocity affected the corrosion mechanism, and the RCE was found to be one of the best practical geometries to accomplish this task. Equations developed by Silverman allowed rotation speeds to be chosen so that the mass transfer coefficients of the RCE would be identical to the modeled geometry.

Ashiru and Farr [27] used the Rotating Disk Electrode (RDE) hydrodynamic technique to provide some kinetic information concerning the electrodeposition of silver from iodide and cyanide electrolytes which were prepared in the laboratory. They found that the RDE technique shed some light on the cathodic discharge current and the associated reaction path during silver deposition. They concluded that the silver electrodeposition study using the RDE technique was more practical than the ordinary method for silver deposition.

Neville et al. [28] conducted an experimental study that used the assessment of the oxygen reduction reaction at a RDE to examine its suitability for scale deposition studies. This method was efficient for studying nucleation and growth of scale on solid surfaces. It was found effective in predicting the scale coverage on the metal surfaces. They confirmed the experimental results by comparing the predicted coverage with that of image analysis, which verified the actual percentage surface coverage by the deposited scale.

The above literature review suggests that the deposition of Calcium Sulfate ($CaSO_4$) on titanium metal was not addressed in detail. However, most heat exchangers used in the corrosive industrial applications are made of titanium metal. Also the use of more economical material, such as coated carbon steel instead of titanium in industrial applications has a tremendous equipment cost reduction impact which was not

evaluated in the literature. Therefore, the present experimental research was done to compare the scale deposition of Calcium Sulfate ($CaSO_4$) on these two different materials, i.e. titanium and coated carbon steel, and to evaluate the scale elimination and cost reduction for both cases.

1.2 Objectives

Calcium Sulfate ($CaSO_4$) is considered to be one of the most commonly found scales in the Arabian Gulf and Red Sea regions. Scale formation reduces the heat transfer, which reduces the whole plant and refinery performance. The objective of this experimental research is to study the deposition and morphology of Calcium Sulfate ($CaSO_4$) scale on coated carbon steel and titanium surfaces tested at different Reynolds numbers by varying the RPM of the rotating cylinder. The economic impact of using coated carbon steel instead of titanium in industrial applications is also investigated. The experiments were conducted in the laboratory of the Research Institute at KFUPM by using Rotating Cylinder Electrode (RCE) apparatus. The RCE is a proven test rig used to simulate the pipe flow. In this experimental study, the heating temperature, sample surface roughness, sample dimensions, solution concentration, experiment and drying time, experiment setup, and motor rotational speed were controlled to measure the deposition rate of Calcium Sulfate ($CaSO_4$).

A literature review was carried out to obtain relevant studies for Calcium Sulfate ($CaSO_4$) scale deposition on different metal surfaces. This review shows that the scale deposition of Calcium Sulfate ($CaSO_4$) on coated carbon steel and titanium metals has not been investigated yet. The economic impact of using coated carbon steel instead of expensive titanium metal in industrial applications has not been

addressed until now. The literature search encouraged the examination of these two types of material in order to evaluate and compare the scale elimination of Calcium Sulfate ($CaSO_4$) and the equipment capital cost reduction for both materials.

CHAPTER 2

EXPERIMENTAL

2.1 Experimental Setup

The Rotating Cylinder Electrode (RCE) is a well established technique for studying kinetics of corrosion [24-26] and electrodeposition [27]. This technique was also used for investigating the scale deposition [29]. The RCE has some advantages over the conventional flow loop for studying the scale buildup, due to simplicity for establishing turbulent flow conditions at lower agitation rates [27], under controlled hydrodynamic conditions.

The RCE used for conducting the experiments in the present study is shown in Figure 2-1. The RCE consists of a supersaturated solution tank, an adjustable speed motor, a Teflon-coated shaft, a Teflon ring, a specimen, a Teflon cap, a glass cell and a hot water circulation bath. Coated carbon steel and titanium samples were fitted to the shaft of the rotating motor. The shaft holding the sample was completely immersed in a double-wall glass cell that contained a supersaturated solution. The supersaturated solution was supplied to the glass cell from a tank. All the experiments were conducted at 60 ˚C temperature and atmospheric pressure.

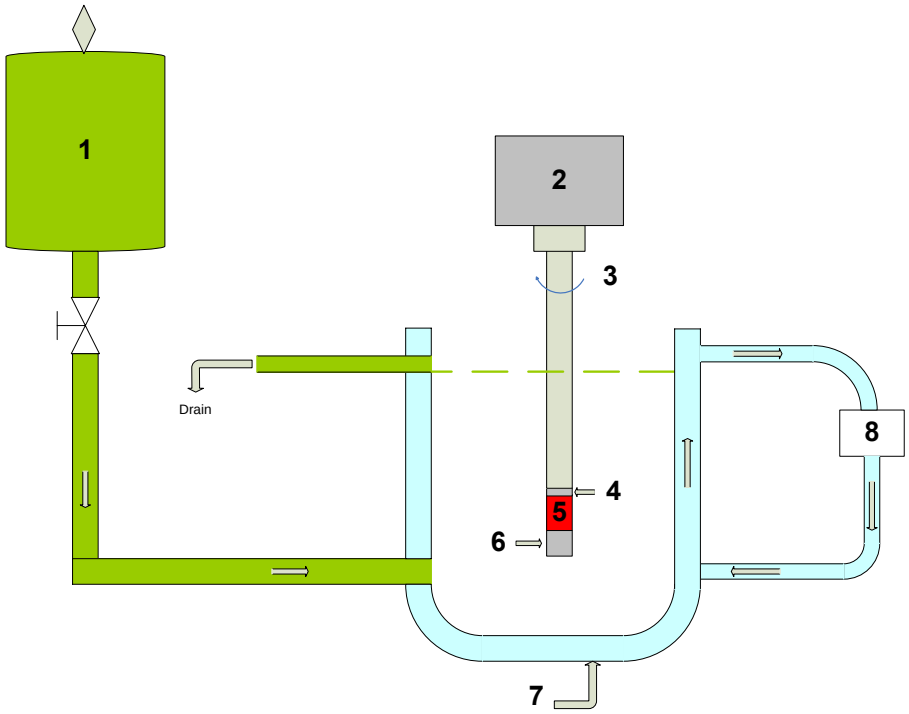

1	Supersaturated solution	5	Specimen
2	Adjustable Speed Motor	6	Teflon cap
3	Teflon-coated shaft	7	Glass cell
4	Teflon ring	8	Hot water circulation bath

Figure 2-1: Schematic of the Experimental Setup of RCE Apparatus

The solution tank which contained Calcium Chloride ($CaCl_2$) and Sodium Sulfate (Na_2SO_4) supersaturated solutions had a volume of four liters. It was connected to the cylindrical double wall glass cell via 6.35 mm tubing. The glass cell was 130 mm long with an inner diameter of 34 mm. The supersaturated solution flowed to the glass cell at a rate of 1.0 to 1.5 liters/hour. Overflow fluid was drained though an outlet of 6.35 mm tubing. Continuous flow of the fresh solution to the glass cell ensured that the test specimen was exposed to a solution of constant composition. The motor speed was adjustable, which enabled the sample rotation speed to be varied from 1 to 9999 RPM. The rotation speeds used in the experiments varied from 100 to 2000 RPM.

At the beginning of each experiment, the supersaturated solution was prepared and put into the supersaturated solution tank (1). The solution was allowed to flow to the glass cell (7) and heated to the required temperature of 60 ˚C by circulating the hot water. The hot water was circulated through the jacket surrounding the cylindrical glass cell. The water in the glass cell was circulated by the use of a constant temperature water-circulating bath arrangement (8) as shown in Figure 2-1. Each experiment was conducted at a certain preset rotational speed and at a temperature of 60 ˚C under atmospheric pressure. The duration selected for each experiment was six hours.

When the supersaturated solution reached a temperature of 60 ˚C and the motor was set to the required rotational speed, the test rig was ready to start. Before starting the experiment, each specimen was thoroughly cleaned with distilled water and acetone, weighed and mounted on the shaft of the rotating equipment. The shaft was immersed in the glass cell, and the test started. At the end of each experiment, the

specimen was rinsed with water and carefully removed from the shaft. It was dried in the oven for two hours. The oven temperature was set at 70 ˚C. Then, the test sample was re-weighed to determine the mass of scale gained by the specimen.

Before starting the next experiment the glass cell and the solution tank were soaked overnight with dilute acid (HCl) and then thoroughly cleaned with normal tap water followed by cleaning with distilled water.

2.2 Preparation of Samples

In this experimental work, two types of materials, namely coated carbon steel and titanium, were used for the tests. The specimens were machined to have a hollow cylindrical shape. The cylindrical test specimens were machined to 12.7 mm long and 12.7 mm in diameter with 0.25 mm tolerance. A central hole of 6.35 mm was drilled in each sample. The dimensions used to fabricate and machine the test specimens are shown in Figure 2-2. The central hole was used to fit the sample onto the Teflon coated shaft of the RCE apparatus. Each sample was securely tightened on the shaft with the help of a Teflon end-cap. Thus the specimen became a part of the long cylindrical shaft of the RCE exposing the peripheral surface of the specimen to the supersaturated solution. The following paragraphs describe the experimental preparation procedure of the coated carbon steel and titanium test specimens.

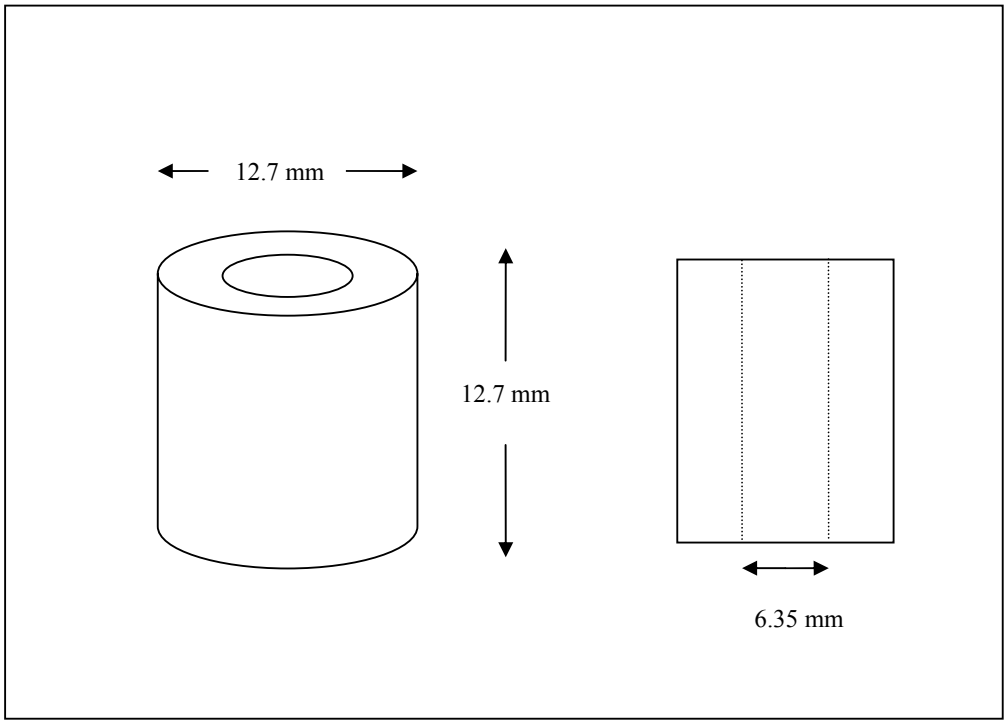

Figure 2-2: Sample Dimensions

For the coated carbon steel, the bare samples were machined from a commercial-grade carbon steel bar. Each sample was machined to the dimensions given in Figure 2-2 with 0.25 mm tolerance. The bare carbon steel samples were coated by Sakaphen GmbH Company in Germany. The coating was applied on the sample external surface by using the Sakaphen Coating Si 57 E. This coating has a phenolic epoxy resin base, and it is characterized by its oxide red color. It is applied on the heat exchanger tubes, the condensers, the evaporators, the water treatment equipment, the salt units and the piping system. It has strong resistance to alkaline or weak acid media, all types of cooling waters, and salt solutions. This coating can be used in service with a pH range between 4.0 and 14. The coating is applied with an approximately 200 micro-meter thick layer, and it can withstand a temperature of 180 ˚C. The overall diameter of the test sample was not affected by the thin layer of the coating. The samples were cleaned thoroughly by degreasing and rinsing them with

distilled water. The roughness of these samples was measured by using the roughness measuring machine available in KFUPM/RI. The measured roughness of the coated carbon steel samples was 20 micro-inch. The coated carbon steel samples are shown in Figures 2-3.

Figure 2-3: Photograph of Coated Carbon Steel Samples

The titanium samples were machined from SB-338 Grade 2 titanium metal bar stock. The samples were machined to the dimensions shown in Figure 2-2 by using a Computerized Numerical Control (CNC) lathe and drilling machines. The titanium samples were fitted on the lathe machine by using a special adapter as shown in Figure 2-4, and then were polished to the desired roughness with 600-grit silicon carbide to obtain a uniform surface roughness of 20 micro-inch similar to the coated carbon steel samples. The titanium surface roughness was measured by using the

Surface Roughness Machine available in KFUPM/RI. The polishing was done by using a lathe machine as shown in Figure 2-5. After polishing, the test specimens were thoroughly degreased with acetone and then rinsed with distilled water. The titanium samples are shown in Figure 2-6.

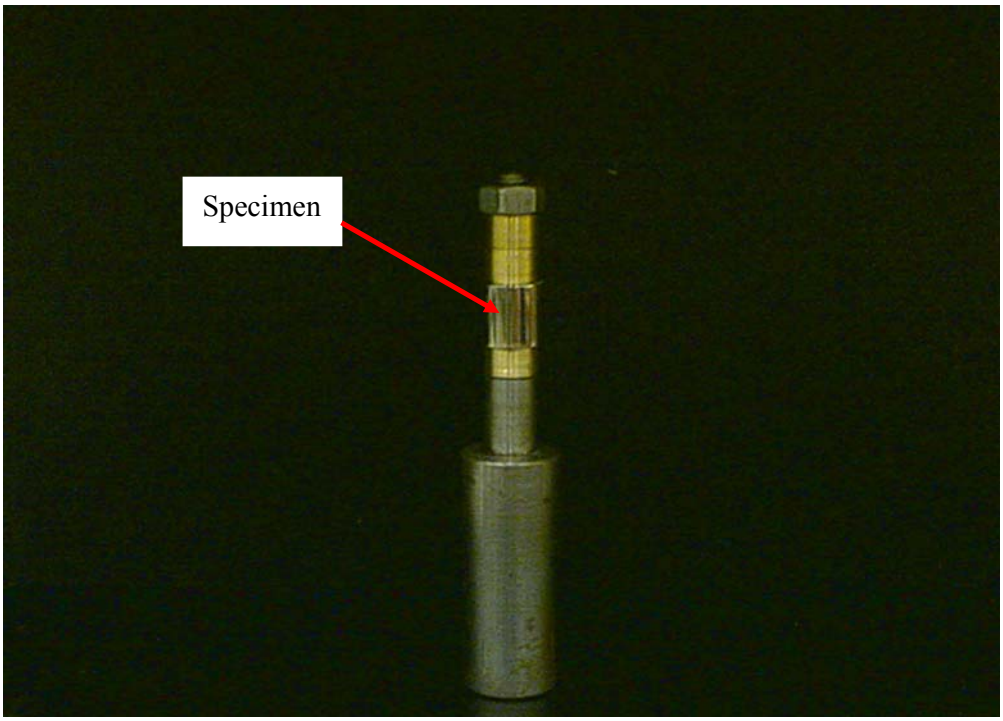

Figure 2-4: Specimen Adaptor used for Polishing Metal Samples

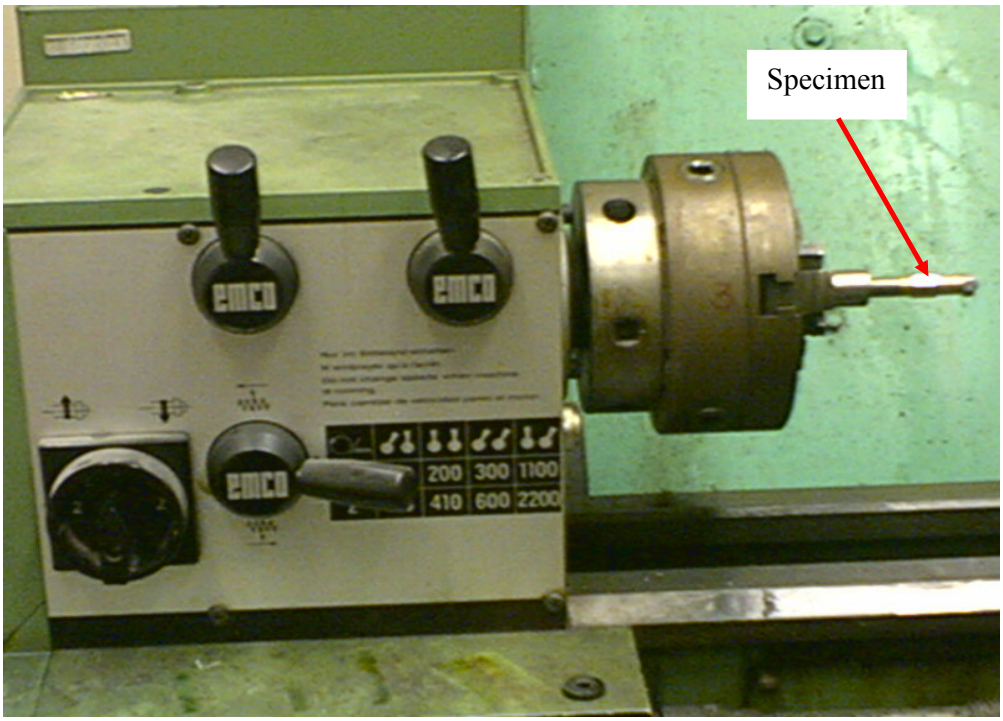

Figure 2-5: Photograph of Lathe Machine Used for Polishing Titanium Samples

Figure 2-6: Photograph of Titanium Samples

2.3 Preparation of Solution

The supersaturated solutions were prepared by using 133.424 g of Calcium Chloride ($CaCl_2$) and 170.448 g Sodium Sulfate (Na_2SO_4) respectively. Each salt was dissolved separately in two 20-liter distilled water bottles. Each salt was mixed carefully to ensure the complete dissolving of the salt. For the test solution, two equal volumes of reactant solutions were mixed together in the solution tank to produce Calcium Sulfate ($CaSO_4$) precipitate, according to the following chemical reaction upon heating:

$$CaCl_2 + Na_2SO_4 \rightarrow CaSO_4 + 2NaCl \qquad (2.1)$$

The mixed supersaturation solutions provided a certain predetermined molarity of 0.03 mole/liter of $CaSO_4$.

2.4 Experimental Procedure

During the experimental work, we used the following procedure.

First, the heater was switched on with the preset heating temperature of 60 ˚C for the hot water circulation bath. It was used to heat the supersaturated solution to a temperature of 60 ˚C. The supersaturated solution was put into the solution tank and allowed to flow to the double-wall glass cell. The glass cell acted as a heat exchanger. The flow of the solution was stopped when the solution level got close to the drain hole of the cell. The solution inside the cell reached the same temperature as the circulating water after almost 15.0 minutes. The test rig is shown in Figure 2-7.

During solution heating, the sample was prepared and cleaned by the procedure mentioned in Section 2.2. After initial weighing, the test specimen was attached to the RCE shaft, and the motor was set to the required speed. After approximately 20 minutes, the solution inside the glass cell reached a steady-state condition. At this stage the shaft was immersed in the solution inside the glass cell, and then the test was started by operating the rotating equipment at a predetermined selected speed. The outlet tubing took the overflow to the drainage. The experiments were monitored closely during the test to take care of any unexpected failures such as solution running out, build-up of scale inside the tube, or drain blockage. The tank and glass cell were cleaned with dilute acid (HCl), normal tap water and distilled water after each run to get rid of any contaminants.

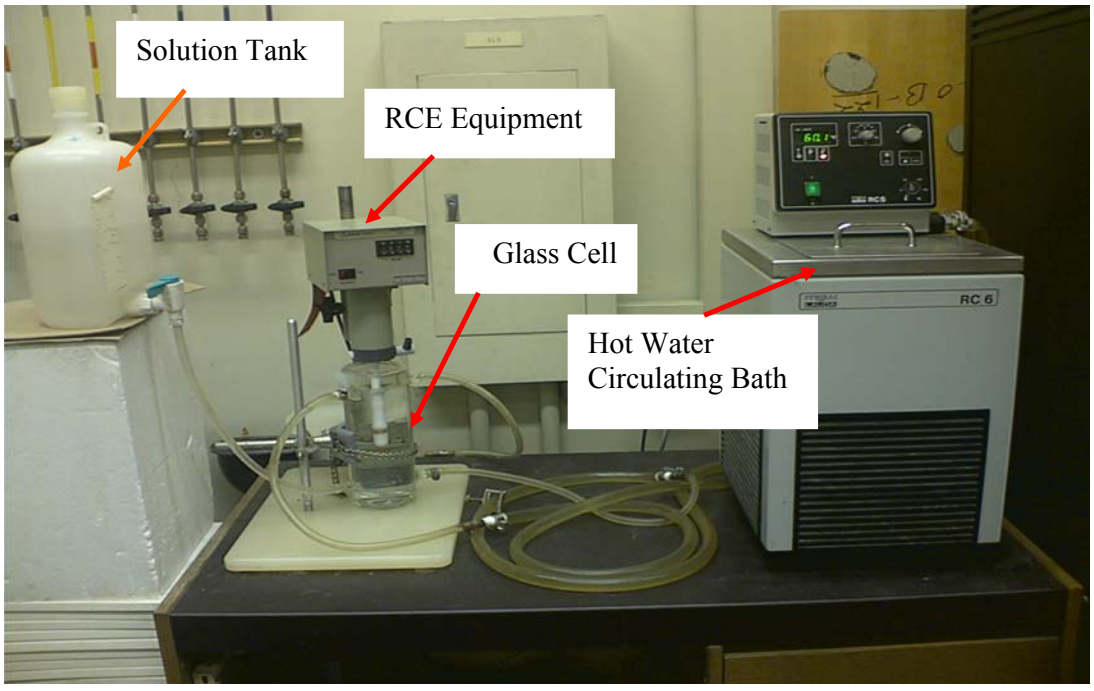

Figure 2-7: Photograph of Apparatus Components

CHAPTER 3

DATA REDUCTION AND UNCERTAINTY ANALYSIS

3.1 Data Reduction Equation

The weight gained (W_g) by the specimen was measured by the weight difference of the specimen after the test and its initial weight before the test. The deposition rate (D_r) was calculated as the weight gained (W_g) of the scaled specimen in grams (g) divided by the surface area of the specimen in square meters (m^2), and the experiment time in hours (hr). The deposition rate (D_r) therefore has units of g. m^{-2}. hr^{-1}.

The Calcium Sulfate ($CaSO_4$) deposition rate on the coated carbon steel and titanium samples was calculated by the following reduction equation.

$$D_r = W_g * A_s^{-1} * t^{-1} \qquad (3.1)$$

where

D_r Deposition rate ($g.m^{-2}.hr^{-1}$)
W_g Weight gained by the specimen (g)
A_s Surface area of the specimen [$\pi * D * L$] (m^2).
t Duration of the experiment work (hr).

For each rotational speed, the equivalent Reynolds numbers (Re) were calculated by using the equation proposed by Gabe [4] which is given as follows.

$$Re = R_1 \omega [(R_2 - R_1)/\nu] \quad (3.2)$$

where

Re Equivalent Reynolds number

R_1 Radius of the rotating specimen (cm)

R_2 Radius of the glass cell (cm)

ω Angular velocity of the rotating specimen (rad/sec)

ν Fluid kinematics viscosity (cm^2/s)

3.2 Uncertainty Analysis

Uncertainty analysis equations used in the experimental work were based on Coleman and Steele [30]. They included the precision, the bias, and the resultant uncertainty. Bias errors were often neglected in books and articles in error analysis or uncertainty analysis by assuming that "all bias errors have been eliminated by calibration". Therefore, the precision uncertainty will be considered here only to calculate the amount of uncertainty in the current experimental work. The method for performing the uncertainty analysis was based on Taylor [31]. His theory for the uncertainty analysis is summarized in the following paragraph.

The uncertainty analysis associated with experimental results is determined by using a data reduction equation. The measurements of the variables (W_g, L, D, and t) have uncertainties associated with them, so that the uncertainties of each individual variable propagate through the data reduction equation into the result.

For the general case in which the experimental result r is a function of J variables X_i is given by the following equation.

$$r = r\,(X_1, X_2, \ldots\ldots, X_J) \tag{3.3}$$

Equation (3.3) is the data reduction equation used for determining r from the measured values of the variables X_i. The uncertainty in the result is given by the following equation.

$$U_r^2 = \left[\left(\frac{\partial r}{\partial X_1} U_{x1}\right)^2 + \left(\frac{\partial r}{\partial X_2} U_{x2}\right)^2 + \ldots\ldots\ldots\ldots + \left(\frac{\partial r}{\partial X_J} U_{xJ}\right)^2\right] \tag{3.4}$$

where

U_{Xi} = the uncertainties in the measured variables X_i

No general discussion of errors can be complete in listing the elements contributing to error in a particular measurement. However, errors are grouped into two very general categories by Figliola [32]. They are as follows.

1. Bias error
2. Precision error.

The total error in a single measurement is the sum of the bias and the precision errors in that measurement. The total error contained in a set of measurements, obtained under seemingly fixed conditions, can be described by an average bias error and a statistical estimate of the precision errors in the measurements.

3.2.1 Uncertainty in Deposition Rate

Reynolds number (Re) and Deposition Rate (D_r) are functions of many parameters. The main contributing parameters are presented by the following equations:

$$\mathrm{Re} = f(R_1, R_2, \omega, \nu) \tag{3.5}$$

$$W_g = f(Re, t, \Delta T\ ) \tag{3.6}$$

Taking into consideration only the measured values which have significant uncertainty, the Deposition rate is a function of

$$D_r = f(\rho, \omega, \Delta T, r, D, L, t, \mu) \tag{3.7}$$

All the variables are measured except the constant pi (π). Re is directly proportional to the weight gain (W_g) and its contribution to the error is apparent, since the process is diffusion-controlled. A simplified form of the reduction equation is as follows:

$$D_r = W_g * (\pi * D * L)^{-1} * t^{-1} \tag{3.8}$$

Now, the standard uncertainty in the deposition rate is calculated by using the following equation.

$$U_{D_r}^2 = \left(\frac{\partial D_r}{\partial W_g} U_{Wg}\right)^2 + \left(\frac{\partial D_r}{\partial D} U_D\right)^2 + \left(\frac{\partial D_r}{\partial L} U_L\right)^2 + \left(\frac{\partial D_r}{\partial t} U_t\right)^2 \tag{3.9}$$

The uncertainty propagation for the dependent variables, in terms of the measured values, is calculated by using the Engineering Equation Solver (EES) software. The measured variables x_1, x_2, etc. have a random variability that is referred to as its uncertainty. The uncertainty is displayed as (a +/- u_x). The input to EES software for calculating the uncertainty of a dependent variable combines the magnitude of the measured variable with the uncertainty in each measured variable.

Figures 3-1 and 3-2 below depict a sample of programming and calculating the uncertainty for the deposition rate (D_r) of each sample by using the EES software.

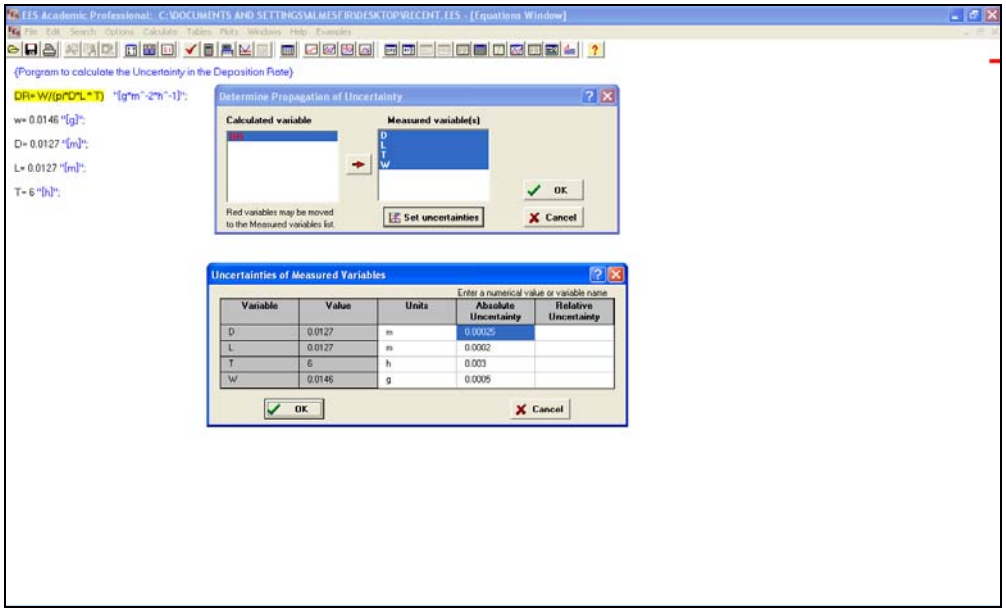

Figure 3-1: Programming the Uncertainty of Deposition Rate (D_r)

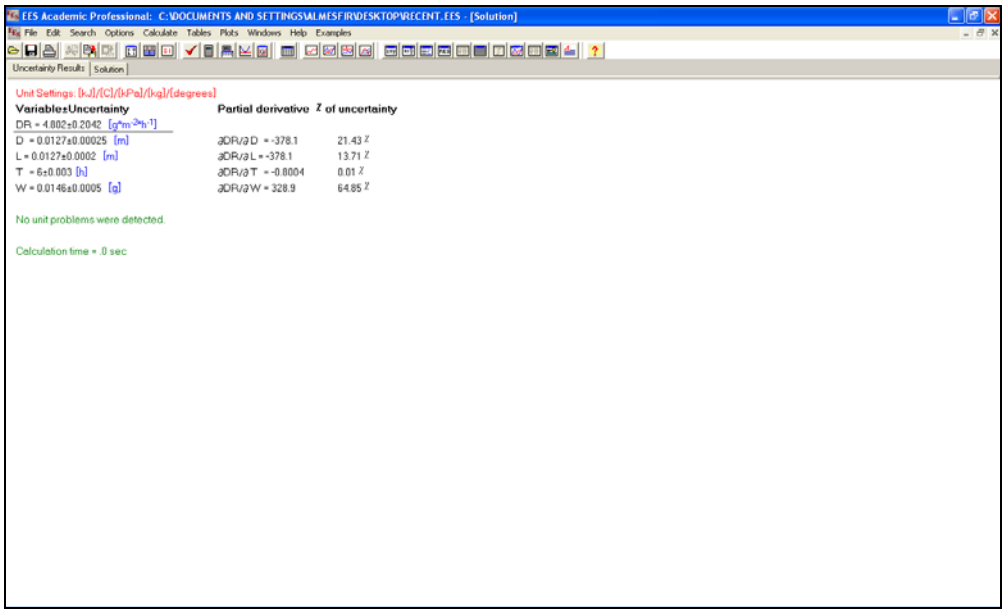

Figure 3-2: Calculating the Uncertainty of Deposition Rate (D_r)

3.3 Uncertainty Calculations

3.3.1 Uncertainty Analysis for Coated Carbon Steel Surfaces

The following tables illustrate the uncertainty analysis for coated carbon steel surfaces at three different rotational speeds. The selected rotational speeds were 100, 1000, and 2000 RPM. These rotational speeds were selected to present the effect of the uncertainty of the main contributing factors, such as specimen diameter (D), length (L), time (t) and gained weight (W_g) on the Calcium Sulfate ($CaSO_4$) deposition rate (D_r).

As shown in Tables 3-1 to 3-3 for coated carbon steel samples, more than 74 % of sensitivity is caused by the weight gain (W_g) of the specimens. The weight Gain (W_g) parameter is affected by many factors such as experimental time, drying time, solution preparation, sample preparation, and sample detachment after the test. The last factor is the main contributor to the final result. If the sample is not removed carefully from the shaft, some of the Calcium Sulfate ($CaSO_4$) scale might be lost, and the test result might not be accurate. The parameter least affecting the deposition rate (D_r) is the experiment time (t) since it represents 0.03 % of the sensitivity result. Specimen diameter (D) and length (L) represent almost 20 % of the sensitivity result. The maximum uncertainty of the deposition rate (D_r) is $\pm$ 12.0 % at the three selected rotational speeds.

Table 3-1: Coated Carbon Steel Uncertainty Analysis for D_r = 37.1037 at 100 RPM and Re= 1457

Variable ± Uncertainty	Partial Derivative	% of Sensitivity
D_r =37.1037 ± 2.845		
D = 0.0127 ± 0.004 (m)	$\partial Dr / \partial D$ = -2292	10.38 %
L = 0.0127 ± 0.00025 (m)	$\partial Dr / \partial L$ = -2292	4.06 %
t = 6 ± 0.008 (hr)	$\partial Dr / \partial T$ = -4.852	0.02 %
W_g = 0.0885 ± 0.0080 (g)	$\partial Dr / \partial W$ = 328.9	85.54 %

Table 3-2: Coated Carbon Steel Uncertainty Analysis for D_r = 34.88 at 1000 RPM and Re= 14567

Variable ± Uncertainty	Partial Derivative	% of Sensitivity
D_r = 34.88 ± 3.055		
D = 0.0127 ± 0. 0004 (m)	$\partial Dr / \partial D$ = -3287	18.52 %
L = 0.0127 ± 0.00025 (m)	$\partial Dr / \partial L$ = -3287	7.24 %
t = 6 ± 0.008 (hr)	$\partial Dr / \partial T$ = -6.957	0.03 %
W_g = 0.1269 ± 0.008 (g)	$\partial Dr / \partial W$ = 328.9	74.21 %

Table 3-3: Coated Carbon Steel Uncertainty Analysis for D_r = 22.2579 at 2000 RPM and Re= 29135

Variable ± Uncertainty	Partial Derivative	% of Sensitivity
D_r =22.2579 ± 2.756		
D = 0.0127 ± 0.0004 (m)	$\partial Dr / \partial D$ = -1733	6.33 %
L = 0.0127 ± 0.00025 (m)	$\partial Dr / \partial L$ = -1733	2.47 %
t = 6 ± 0.008 (hr)	$\partial Dr / \partial T$ = -3.667	0.01 %
W_g = 0.0669 ± 0.008 (g)	$\partial Dr / \partial W$ = 328.9	91.19 %

3.3.2 Uncertainty Analysis for Titanium Surfaces

The following tables illustrate the uncertainty analysis for titanium surfaces at three different rotational speeds. The selected rotational speeds were 100, 1000, and 2000 RPM. These speeds present the effect of uncertainty of the main contributing factors, such as specimen diameter (D), length (L), time (t) and weight gain (W_g) on the deposition rate (D_r) of Calcium Sulfate ($CaSO_4$).

As shown in Tables 3-4 to 3-6 for Titanium samples, more than 73 % of the sensitivity is caused by the specimen weight gain (W_g). The weight gain (W_g) parameter is affected by many factors such as experimental time, drying time, solution preparation, sample preparation, and sample removal after the test. The last factor is the main contributor to the final result. If the sample is not removed carefully from the shaft, some of the Calcium Sulfate ($CaSO_4$) scale might be lost, and the test result might not be accurate. The parameter least affecting the deposition rate (D_r) is the experiment time (t) since it represents 0.07 % of the sensitivity result. Specimen diameter (D) and length (L) represent almost 25 % of the sensitivity result. The maximum uncertainty of the deposition rate (D_r) is $\pm$ 6.0 % at the three rotational speeds.

The uncertainty percentage of the deposition rate is reduced by half for the titanium samples compared to coated carbon steel. This is due to the nature of the scale accumulation on these two metals. For coated carbon steel, the scale did not adhere strongly to the surface, and it had a spongy shape, which fell off easily during the samples' detachment. However, the scale adhering to the titanium had a compact

scale shape, which reduced the possibility of the scale being lost during the sample' removal.

Table 3-4: Titanium Uncertainty Analysis for D_r = 49.1096 at 100 RPM and Re= 1457

Variable ± Uncertainty	Partial Derivative	% of Sensitivity
D_r =49.1096 ± 3.062		
D = 0.0127 ± 0.0004 (m)	$\partial Dr / \partial D$ = -3318	18.78 %
L = 0.0127 ± 0.00025 (m)	$\partial Dr / \partial L$ = -3318	7.34 %
t = 6 ± 0.008 (hr)	$\partial Dr / \partial T$ = -7.022	0.03 %
W_g = 0.1281 ± 0.008 (g)	$\partial Dr / \partial W$ = 328.9	73.85 %

Table 3-5: Titanium Uncertainty Analysis for D_r = 67.4198 at 1000 RPM and Re= 14567

Variable ± Uncertainty	Partial Derivative	% of Sensitivity
D_r =67.4198 ± 3.076		
D = 0.0127 ± 0.0004 (m)	$\partial Dr / \partial D$ = -3375	19.26 %
L = 0.0127 ± 0.00025 (m)	$\partial Dr / \partial L$ = -3375	7.52 %
t = 6 ± 0.008 (hr)	$\partial Dr / \partial T$ = -7.143	0.03 %
W_g = 0.1303 ± 0.008 (g)	$\partial Dr / \partial W$ = 328.9	73.18 %

Table 3-6: Titanium Uncertainty Analysis for D_r = 80.11 at 2000 RPM and Re= 29135

Variable ± Uncertainty	Partial Derivative	% of Sensitivity
D_r =80.11 ± 3.954		
D = 0.0127 ± 0.0004 (m)	$\partial Dr / \partial D$ = -6252	40.01 %
L = 0.0127 ± 0.00025 (m)	$\partial Dr / \partial L$ = -6252	15.63 %
t = 6 ± 0.008 (hr)	$\partial Dr / \partial T$ = -13.23	0.07 %
W_g = 0.2414 ± 0.008 (g)	$\partial Dr / \partial W$ = 328.9	44.29 %

CHAPTER 4

RESULTS AND DISCUSSION

4.1 Experimental Findings

Many factors affect the deposition of Calcium Sulfate ($CaSO_4$) scale on coated carbon steel and titanium materials. Motor speed, solution preparation, solution mixing, sample dimensions, test duration, sample cleaning and dismantling after the test are some of these main factors affecting the deposition buildup and the final results. Some of these factors can be controlled, such as the sample dimensions and the test duration.

The rotational speed and the mixing of the solution had a strong influence on the rate of Calcium Sulfate ($CaSO_4$) scale deposition on metal surfaces. For example, as the rotational speed increased, the rate of mass transport of the scale to the electrode surface increased. This process yielded a quantitative amount of scale deposited on the samples' surface.

The collected data was analyzed to show the effect of the solution hydrodynamic at different rotational speeds on the deposition rate of Calcium Sulfate ($CaSO_4$). For each rotational speed, the equivalent Reynolds number (Re) was calculated by using equation 4.1 proposed by Gabe [4] as follows:

$$Re = R_1 \omega [(R_2 - R_1)/\nu] \quad \textbf{(4.1)}$$

Calcium Sulfate ($CaSO_4$) deposition rate on coated carbon steel and titanium samples was calculated by the following reduction equation.

$$D_r = W_g * A_s^{-1} * t^{-1} \quad \textbf{(4.2)}$$

where

D_r Deposition rate ($g.m^{-2}.hr^{-1}$)
W_g Weight gained by the specimen (g)
A_s Surface area of the specimen [$\pi * D * L$] (m^2).
t Duration of the experiment (hr).

4.1.1 Scale Deposition Rate Results on Coated Carbon Steel

The experimental results of the Calcium Sulfate ($CaSO_4$) deposition rate on coated carbon steel surfaces are shown in Table 4-1. For a given rotational speed, the Reynolds number (Re) was calculated from Equation 4.1, and the deposition rate at a given rotational speed and Reynolds number (Re) was calculated from Equation 4.2. Table 4-1 shows clearly that the deposition rate for coated carbon steel is almost constant, with little increase or decrease corresponding to the increase in rotational speed. Table 4-1 shows also the average value of the three repeated tests of the Calcium Sulfate ($CaSO_4$) scale deposition rate on the coated carbon steel samples.

The deposition rates shown in Table 4-1 are fluctuating, since at a low Reynolds number (Re) the scale is soft and spongy. Low rotational speed and scale gravity

force cause some of the outside deposit layers of the accumulated scale to fall off, which caused a low scale value. However, at a high Reynolds number (Re) the scale accumulated in a more compact manner, and more weight was gained. The behavior of the scale formation (i.e. soft and spongy scale, scale roughness) therefore affected the deposition rate. The values of the deposit rate were fluctuating, as illustrated in Table 4-1.

Table 4-1: Scale Deposition Rate (D_r) for Coated Carbon Steel

Sr. #	Speed (RPM)	Equivalent Re	Scale Deposition Rate (D_r) ($g\ m^{-2}\ h^{-1}$)			Average D_r ($g\ m^{-2}\ h^{-1}$)
			Set # 1	Set # 2	Set # 3	
1	100	1457	30.2769	37.1037	43.2445	36.8750
2	250	3642	24.6529	24.2830	25.4196	24.7852
3	500	7284	37.7736	27.3031	28.2169	31.0979
4	750	10926	30.4577	31.1162	33.4256	31.6665
5	1000	14567	34.8800	42.0807	38.2897	38.4168
6	1250	18209	35.3506	32.7380	30.5199	32.8695
7	1500	21851	35.3057	30.0932	37.0101	34.1363
8	1750	25493	38.2171	35.1107	36.3688	36.5655
9	2000	29135	24.0100	22.2579	26.9355	24.4011

The tabulated experimental results shown above are represented in Figure 4-1 to study the Calcium Sulfate ($CaSO_4$) deposition rate on coated carbon steel. The tests were repeated three times to check the accuracy and uncertainty of the measured value for coated carbon steel surfaces.

Three sets shown in Table 4-1 are presented by graphs showing the value of the deposition rate versus the Reynolds number (Re). Each set compares the deposition

rate on coated carbon steel metal versus the same the Reynolds number (Re). The set shows the actual graph, followed by the best linear fit, and finally the logarithmic best fit curve. The average scale deposition rate of the Calcium Sulfate ($CaSO_4$) is also drawn versus the Reynolds number (Re) for coated carbon steel metal.

Figure 4-1 is for coated carbon steel samples. Each graph shows three repetitions to compare the deposition rate at the same Re (or rotational speed in RPM). These three tests are presented by Set 1, Set 2 and Set 3 respectively.

Figure 4-1 shows the Calcium Sulfate ($CaSO_4$) deposition rate on coated carbon steel. As shown by this figure, the three curves are almost identical. Therefore, at the same Reynolds number (Re) the coated carbon steel sets have almost the same deposition rate as Calcium Sulfate ($CaSO_4$). The deposition rate of Calcium Sulfate ($CaSO_4$) at certain Re increased slightly with +/- 3 % differences, which was an insignificant increase. These differences resulted from the experimental uncertainty. As shown by the uncertainty analysis presented in Section 3.3.1, 74 % of uncertainty is caused by the specimen weight gain (W_g) and the error in the deposition rate does not exceed 12.0 %. The weight gain (W_g) parameter is affected by many factors such as experimental time, drying time, solution preparation, sample preparation, and sample detachment after the test. Therefore, the deposition rate profiles are constant and identical as the Reynolds number (Re) increases.

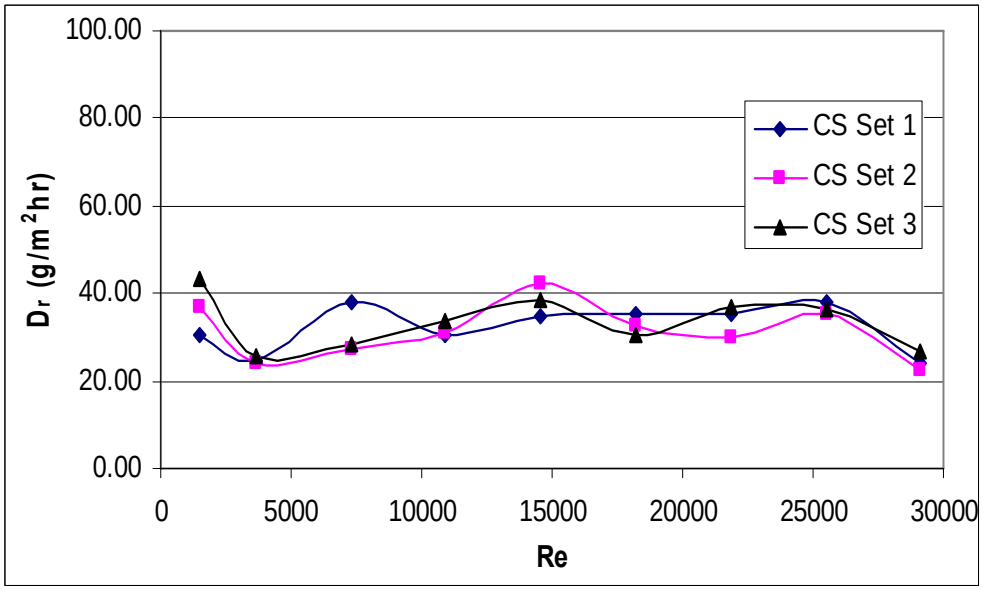

Figure 4-1: Deposition Rate on Coated Carbon Steel for Three Sets

4.1.2 Scale Deposition Rate Results on Titanium

The experimental results for the Calcium Sulfate ($CaSO_4$) deposition rate on titanium surfaces are shown in Table 4-2. For a given rotational speed, the Reynolds number (Re) was calculated from Equation 4.1, and the deposition rate at a given rotational speed and Reynolds number (Re) was calculated from Equation 4.2. The table shows that the deposition rate increases directly with the increase in speed. Table 4-2 shows also the average value of the three repeated tests for the Calcium Sulfate ($CaSO_4$) scale deposition rate on the titanium samples.

The titanium samples attracted more scale than did the coated carbon steel at the same rotational speed. The results of the calculated deposition rate for titanium are also fluctuating within an acceptable range. At some values of the Reynolds number (Re), the shear forces reach a value at which the strength of the outer deposit layers cannot

withstand the increased shear forces. Under these circumstances, the deposition buildup rate is balanced by the removal rate.

Table 4-2: Scale Deposition Rate (D_r) for Titanium

Sr. #	Speed (RPM)	Equivalent Re	Scale Deposition Rate (D_r) ($g\ m^{-2}\ h^{-1}$)			Average D_r ($g\ m^{-2}\ h^{-1}$)
			Set # 1	Set # 2	Set # 3	
1	100	1457	47.1939	49.1096	45.6731	47.32553
2	250	3642	60.4936	63.0725	62.6152	62.06043
3	500	7284	50.1046	54.9306	48.6083	51.2145
4	750	10926	74.4258	78.1407	75.4881	76.0182
5	1000	14567	55.1311	48.0044	67.4198	56.85177
6	1250	18209	72.3566	75.6733	84.6247	77.55153
7	1500	21851	76.3518	67.7514	81.7143	75.2725
8	1750	25493	75.2302	71.1776	70.8625	72.42343
9	2000	29135	88.9352	80.1100	86.0247	85.0233

Figure 4-2 is for titanium samples. Each graph shows three repetitions to compare the deposition accumulation at the same Re (or rotational speed in RPM). These three tests are presented by Set 1, Set 2 and Set 3 respectively.

Figure 4-2 shows a set of three curves for the Calcium Sulfate ($CaSO_4$) deposition rate on the titanium test specimens. Each test was repeated three times to verify and compare the deposition rate of Calcium Sulfate ($CaSO_4$) on these samples. As shown by this figure, the three curves are almost identical. Therefore, at the same Reynolds number (Re) these three sets have almost the same deposition rate as Calcium Sulfate ($CaSO_4$). At certain values of the Reynolds number (Re), the Calcium Sulfate

($CaSO_4$) deposition rate varies with +/- 6 % differences. These differences resulted from the experimental uncertainty.

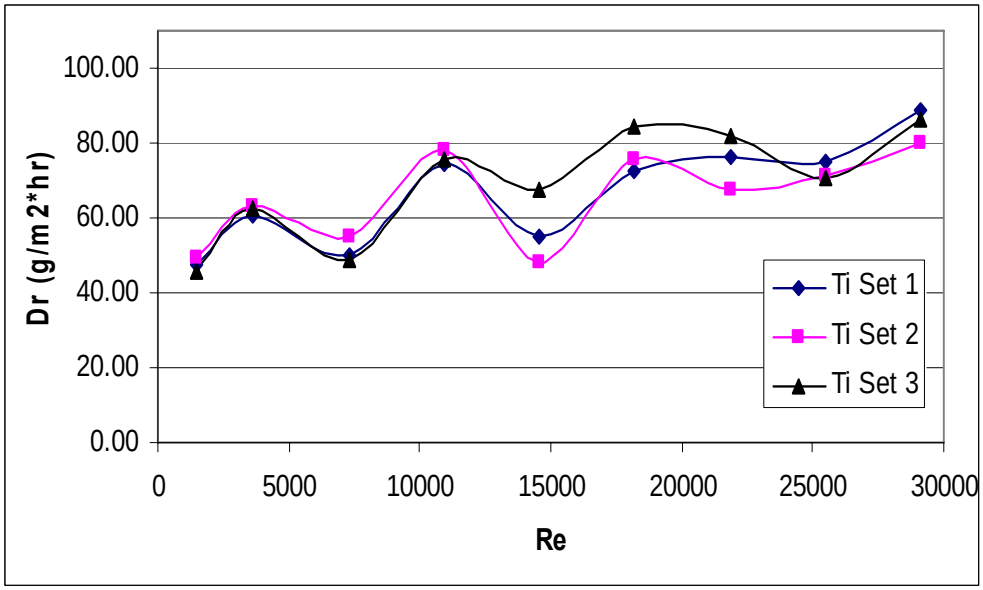

Figure 4-2: Deposition Rate on Titanium for Three Sets

4.1.3 Comparison of Scale Deposition on Coated Carbon Steel and Titanium

Figure 4-3 shows the best fitted straight lines for the Calcium Sulfate ($CaSO_4$) deposition rate on both coated carbon steel and titanium samples. It is clear from this figure that the Calcium Sulfate ($CaSO_4$) deposition rate increases more as the Reynolds number (Re) increases for the titanium samples, but it increases slightly for the coated carbon steel samples.

The average values for the Calcium Sulfate ($CaSO_4$) deposition rate of the three sets were calculated for both coated carbon steel and titanium surfaces. The average deposition rate versus the Reynolds number (Re) is presented for both metals in the following paragraphs.

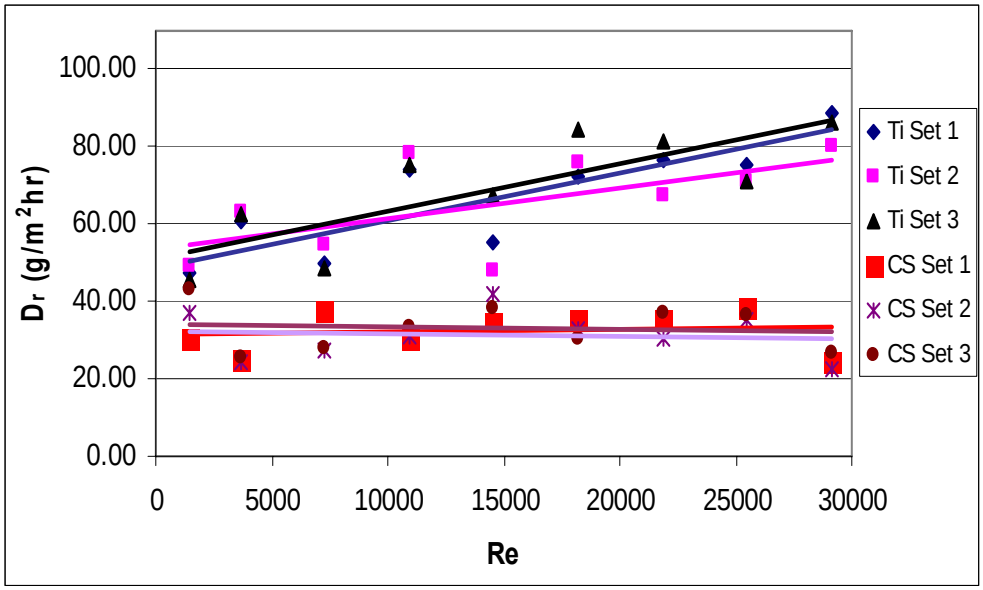

Figure 4-3: Linear Best Fit in Deposition Rate on Coated Carbon Steel and Titanium Metals

Respectively on both coated carbon steel and titanium metals Figures 4-4 and 4-5 show the best fitted straight lines for the average Calcium Sulfate ($CaSO_4$) scale and the logarithm of the average Calcium Sulfate ($CaSO_4$) deposition rate versus the logarithm of the Reynolds number (Re). These curves also show that the Calcium Sulfate ($CaSO_4$) deposition rate increases more as the Reynolds number (Re) increases for the titanium samples, but it increases slightly for the coated carbon steel samples.

As shown in the preceding graphs for the Calcium Sulfate ($CaSO_4$) deposition rate on coated carbon steel and titanium surfaces, the coating on the carbon steel samples reduced the scale buildup and the scale accumulation on the external surfaces of the samples. The curve for the coated carbon steel in Figure 4-4 is almost constant, which indicates that the rate of the scale buildup is equal to the rate of its removal. However, in the titanium samples, the scale growth was significantly more as the rotational speed was increased. Therefore, the coated carbon steel samples showed better resistance to scale deposition compared to the titanium samples. This is clearly illustrated by Figure 4-4 which shows a sharp increase in the Calcium Sulfate ($CaSO_4$) deposition rate on the titanium surfaces and an almost constant deposition rate on the coated carbon steel samples.

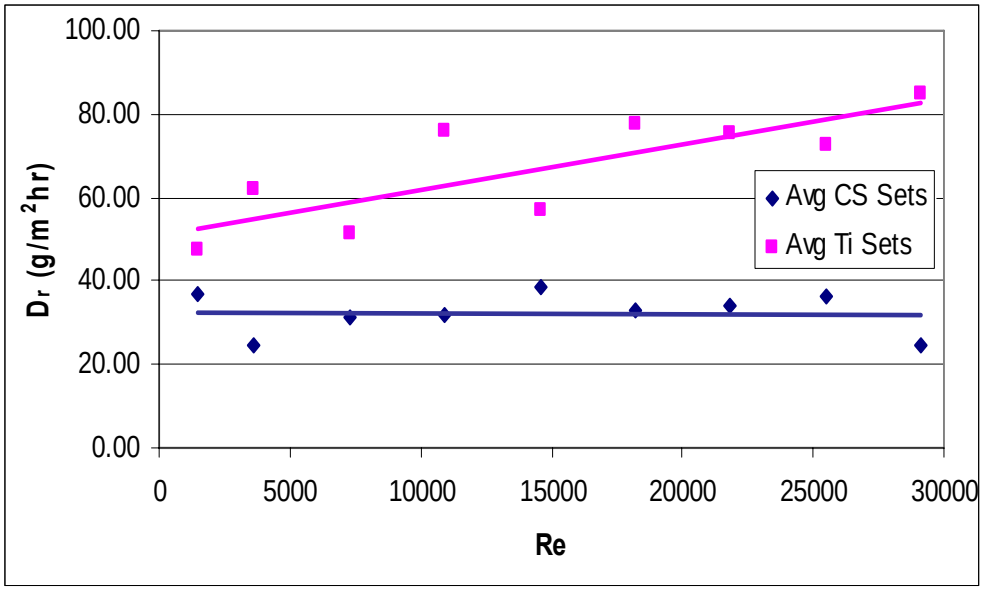

Figure 4-4: Average Linear Best Fit in Deposition Rate on Coated Carbon Steel and Titanium Metals

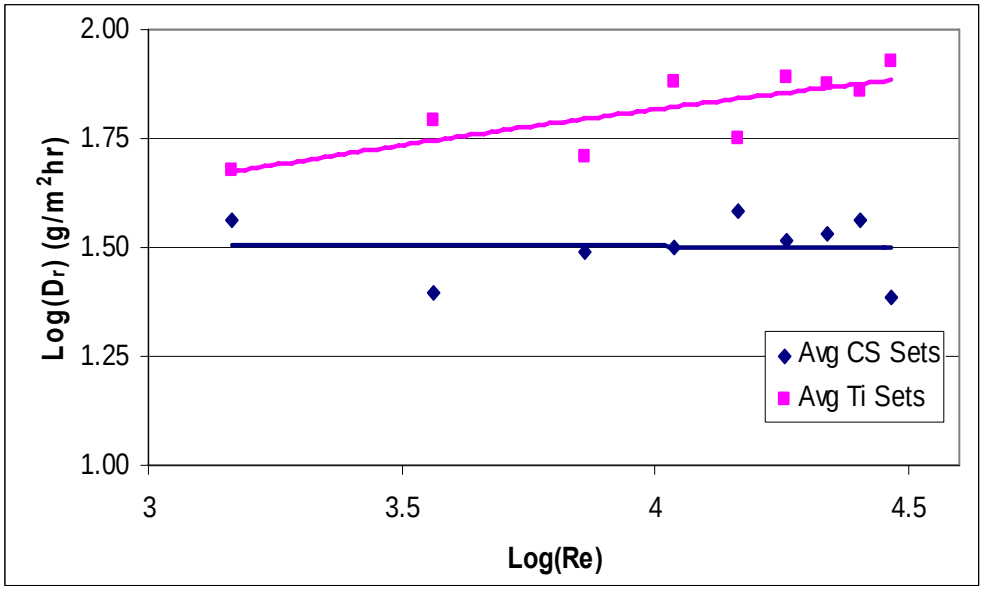

Figure 4-5: Average Linear Best Fit in Logarithm (Deposition Rate) vs. Logarithm (Re)

According to the analysis done by Levich [34], the mass transfer coefficient should increase with the square root of the Reynolds number - $(Re)^{0.5}$. For such cases, the log-log plot should give a straight line with a theoretical slope of 0.5. It is obvious from Figure 4-5 that the log-log plot of the deposition rate (D_r) versus the Reynolds number (Re) shows a linear relationship i.e. a straight line with a slope of 0.45. This result is in close agreement with the theoretically predicted value of 0.5, obtained when the mass transfer coefficient is proportional to the square root of the Reynolds number. This shows that the process is diffusion-controlled.

4.1.4 Photographic Record of Scale Deposition on Coated Carbon Steel Samples

The following photographs show the Calcium Sulfate ($CaSO_4$) deposition on coated carbon steel samples rotated at different speeds ranging from 100 to 2000 RPM.

Figure 4-6 shows the Calcium Sulfate ($CaSO_4$) scale deposition on a coated carbon steel sample rotated at 100 RPM. The scale was uniformly distributed all over the specimen, and it did not adhere firmly to the surface of the sample. The scale looked spongy with a 3 mm thickness. The Reynolds number corresponding to the 100 RPM speed of rotation is approximately 1457, which corresponds to laminar flow.

As the speed of rotation increased, the scale deposition pattern over the specimen surface changed. The scale deposition was scattered, and its thickness changed as the rotational speed varied. The distribution of the scale concentrated at the edges of the sample. Figure 4-7 clearly illustrated this observation for 250 RPM. As shown by this figure, some of the scale started accumulating at the top and bottom of the test specimen. The scale thickness decreased at the center to approximately 2.5 mm.

For the next higher rotational speed of 500 RPM, the weight gained by the sample was more than that for 250 RPM. The scale deposition pattern did not differ much from that of 250 RPM but it was more compact than at the previous speed, which justified the higher weight gained, as can be noticed from Figure 4-8.

Figure 4-9 shows the Calcium Sulfate ($CaSO_4$) scale deposition behavior on a coated carbon steel sample rotated at 750 RPM. Some locations had less deposition than others, and the deposition was not uniform over the entire surface of the specimen.

The scale was soft and it looked spongy. It did not adhere very well to the surface of the specimen, and it could be easily removed. The scale thickness was approximately 1.0 mm at the center and 2.0 mm at the top and bottom sides of the specimen. As the speed of rotation increased, the gained weight increased also.

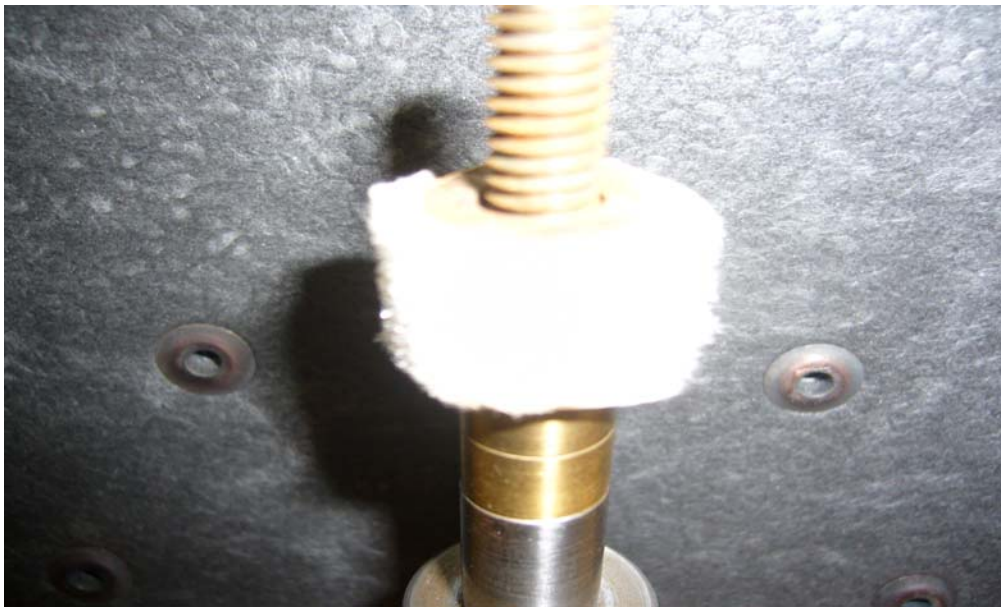

Figure 4-6: Photograph Showing Scale Deposition on Coated Carbon Steel at 100 RPM

Figure 4-7: Photograph Showing Scale Deposition on Coated Carbon Steel at 250 RPM

Figure 4-8: Photograph Showing Scale Deposition on Coated Carbon Steel at 500 RPM

Figure 4-9: Photograph Showing Scale Deposition on Coated Carbon Steel at 750 RPM

Figure 4-10 shows the deposition of Calcium Sulfate ($CaSO_4$) on a coated carbon steel sample rotated at 1000 RPM. The scale adhered more to this sample, compared to the previous cases. The distribution of the scale differed in this case. Most of the scale accumulated at the top and bottom of the sample, but little scale accumulated at its center. At the center, some parts were not covered completely with scale and so the base surface of the sample was seen clearly. The scale was less spongy, and its average thickness was approximately 1.0 mm.

Figure 4-11 shows the deposition of Calcium Sulfate ($CaSO_4$) on a coated carbon steel sample rotating at 1250 RPM. The scale adhered more to this sample than the previous case. Most of the scale accumulated at the top and bottom of the sample, little scale accumulated at its center. The scale in this case was less spongy compared with previous cases. The average thickness of the scale was 1.0 mm.

Figure 4-10: Photograph Showing Scale Deposition on Coated Carbon Steel at 1000 RPM

Figure 4-11: Photograph Showing Scale Deposition on Coated Carbon Steel at 1250 RPM

Figure 4-12 shows the deposition of Calcium Sulfate ($CaSO_4$) on a coated carbon steel sample rotated at 1500 RPM. The scale adhered strongly to this sample. Most of the scale accumulated at the top and bottom of the sample, little scale accumulated at its center. At the center, some parts were not covered completely with scale and so the base surface of the sample was seen clearly. The scale in this case was less spongy than the previous case. The average thickness of the scale was approximately 1.0 mm.

Figure 4-13 shows the deposition of Calcium Sulfate ($CaSO_4$) on a coated carbon steel sample rotated at 2000 RPM. The scale adhered strongly to this sample. The scale accumulated at the top and bottom of the sample, but its center was not covered completely with scale and so the base surface of the sample was seen clearly. The scale in this case was less spongy than the previous case. The scale was uniformly distributed at the top and bottom with 2.0 mm average thickness.

Figure 4-12: Photograph Showing Scale Deposition on Coated Carbon Steel at 1500 RPM

Figure 4-13: Photograph Showing Scale Deposition on Coated Carbon Steel at 2000 RPM

4.1.5 Photographic Record of Scale Deposition on Titanium Samples

The following figures show the pictorial representation of the Calcium Sulfate ($CaSO_4$) deposition on titanium samples obtained at different rotational speeds ranging from 100 to 2000 RPM.

Figure 4-14 shows the Calcium Sulfate ($CaSO_4$) scale deposition on a titanium sample rotated at 100 RPM. The scale was uniformly distributed all over the specimen, and it did not adhere firmly to the surface of the sample. The scale looked spongy, with approximately 5.0 mm thickness. The Reynolds number corresponding to the above speed of rotation is approximately 1457, which is corresponding to a laminar flow

regime. The scale on this titanium sample was thicker by 2.0 mm than that accumulated on the coated carbon steel under the same test conditions.

Figure 4-14: Photograph Showing Scale Deposition on Titanium at 100 RPM

The scale deposition rate and pattern covering the test specimen changed as the speed of rotation increased. The distribution of the scale started concentrating at some locations, such as the edges of the sample. Figure 4-15 clearly illustrates this observation for 250 RPM. As shown by this figure, some of the scale started accumulating more at the top and bottom of the test specimen, but the scale thickness decreased at the center to approximately 3.0 mm. The scale uniformly covered the specimen surface with a soft and spongy pattern. The scale weight increased by 14.73 g compared with the preceding speed. The scale on the titanium sample was thicker by 1.0 mm than that accumulated on the coated carbon steel under the same test conditions.

Figure 4-15: Photograph Showing Scale Deposition on Titanium at 250 RPM

For the next higher rotational speed of 500 RPM, the scale deposition pattern did not differ much from the previous RPM except that it was more compact. More scale accumulated at the bottom and top sides of the sample compared with the previous case. The scale deposition rate on the titanium sample was higher than that on the coated carbon steel conducted under the same experimental conditions. Figure 4-16 shows the Calcium Sulfate ($CaSO_4$) deposition on a titanium sample rotated at 500 RPM.

Figure 4-17 shows the Calcium Sulfate ($CaSO_4$) scale deposition on a titanium sample rotated at 750 RPM. This figure clearly depicts the non-uniform deposition over the entire surface of the specimen. The scale adhering to the surface of the test specimen was soft and spongy. The scale thickness was 1.0 mm at the center and 2.0 mm at the top and bottom sides of the specimen. As the speed of rotation increased, the weight increased also. The scale weight increased by 24.80 g compared with the preceding

speed. The scale on the titanium sample was thicker by 2.0 mm than that accumulated on the coated carbon steel under the same test conditions.

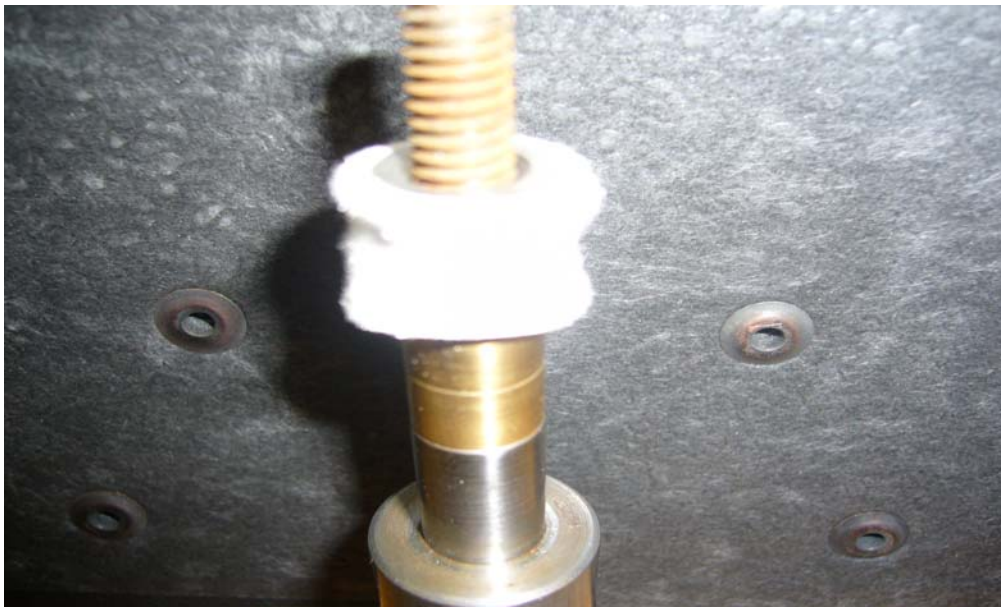

Figure 4-16: Photograph Showing Scale Deposition on Titanium at 500 RPM

Figure 4-17: Photograph Showing Scale Deposition on Titanium at 750 RPM

Figure 4-18 shows the deposition of Calcium Sulfate ($CaSO_4$) on a titanium sample. The test was conducted at 1000 RPM. The scale adhered more to the test sample compared to the previous cases. The distribution of the scale differed in this case. Most of the scale accumulated at the top and bottom of the sample, little scale accumulated at its center. At the center, some parts were not covered completely with scale and so the base surface of the sample was seen clearly. The scale in this case was less spongy compared with previous cases. The average thickness of the scale was approximately 2.0 mm. The scale on the titanium sample was thicker by 1.0 mm than that accumulated on the coated carbon steel under the same test conditions.

Figure 4-19 shows the deposition of Calcium Sulfate (CaSO4) on a titanium sample rotated at 1250 RPM. The scale adhered to the test sample more than the previous case. Most of the scale accumulated at the top and bottom of the sample, little scale accumulated at its center. The scale in this case was less spongy compared with previous cases. The average thickness of the scale was 2.0 mm. The scale weight increased by 20.70 g compared with the preceding speed.

Figure 4-20 shows the Calcium Sulfate ($CaSO_4$) deposition on a titanium sample rotated at 1500 RPM. The scale distribution on this titanium sample was close to that of 1250 RPM. Most of the scale accumulated at the top and bottom sides of the sample, little scale accumulated at its center. The scale in this case was less spongy, and its average thickness was 2.0 mm.

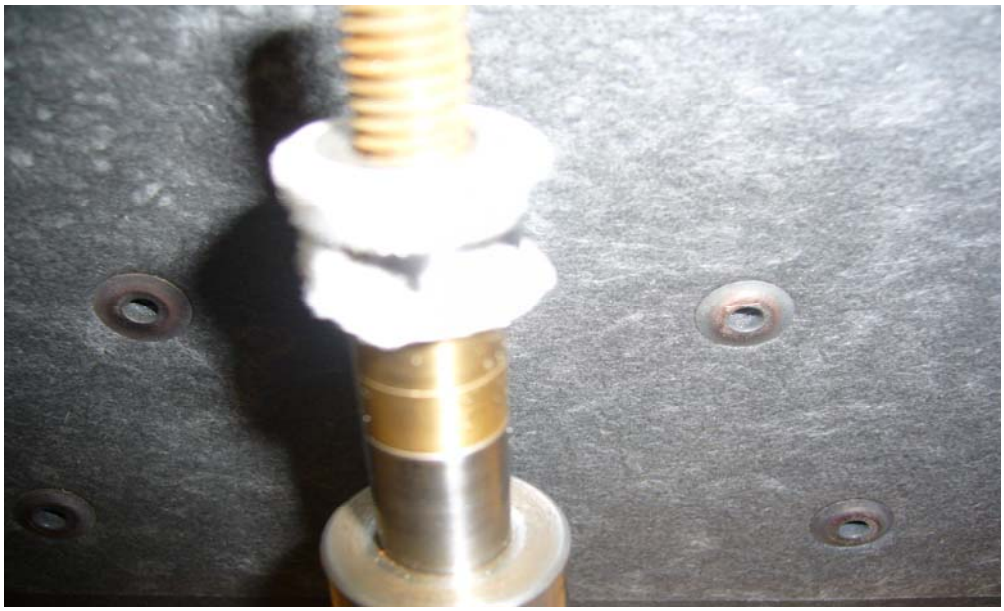

Figure 4-18: Photograph Showing Scale Deposition on Titanium at 1000 RPM

Figure 4-19: Photograph Showing Scale Deposition on Titanium at 1250 RPM

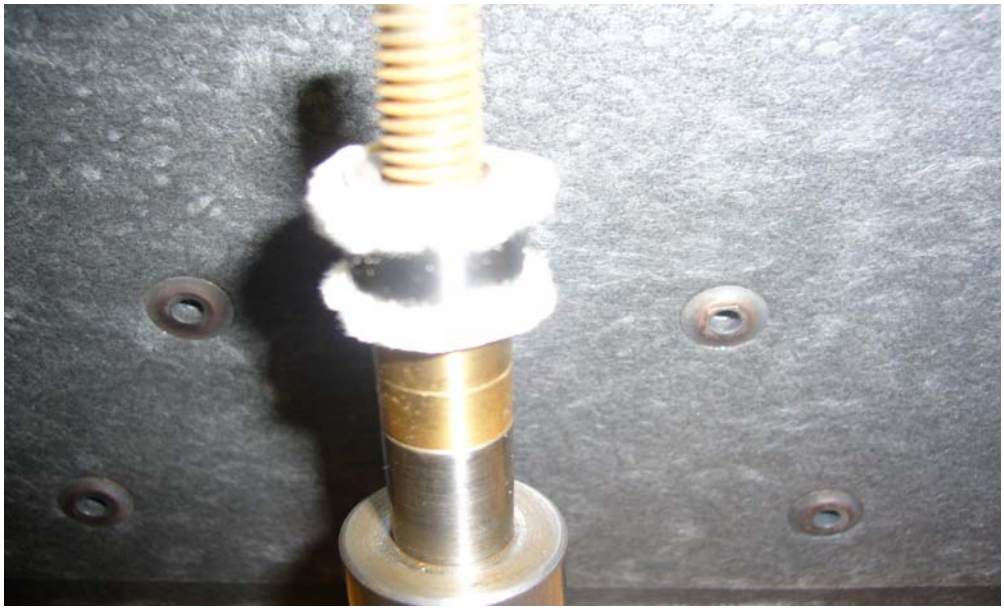

Figure 4-20: Photograph Showing Scale Deposition on Titanium at 1500 RPM

Figure 4-21 shows the deposition of Calcium Sulfate ($CaSO_4$) on a titanium sample rotated at 1750 RPM. The scale adhered strongly to the test sample. Most of the scale accumulated at the top and bottom of the sample, little scale accumulated at its center. At the center, some positions were not covered completely with scale and so the base surface of the sample was seen clearly. The scale in this case was less spongy. Its average thickness was 2.0 mm. The scale on the titanium sample was thicker by 1.0 mm than that accumulated on the coated carbon steel under the same test conditions.

Figure 4-22 shows the deposition of Calcium Sulfate (CaSO4) on a titanium sample rotated at 2000 RPM. The scale adhered strongly to the test sample. The scale accumulated at the top and bottom of the sample, but its center was not covered

completely with scale and so the base surface of the sample was seen clearly. The scale in this case was less spongy than the previous case. The scale was uniformly distributed at the top and bottom with 2.0 mm average thickness. The scale weight increased by 12.60 g compared with the preceding speed.

Figure 4-21: Photograph Showing Scale Deposition on Titanium at 1750 RPM

Figure 4-22: Photograph Showing Scale Deposition on Titanium at 2000 RPM

Figures 4-6 to 4-22 show the effect of the solution hydrodynamic on the Calcium Sulfate ($CaSO_4$) precipitation on coated carbon steel and titanium cylinder specimens. The lower speed of rotation caused lighter, less compact and easily removable scale. As the speed went up, the scale become more compact, and it attached strongly to the upper and lower ends of the metal surfaces, which justified the higher weight gain.

The results of this experimental work indicate that the deposition process is diffusion-controlled. As the speed of rotation increased, more scale was deposited on the metal surface. These results are in agreement with the observation by Quddus and Allam [11] for the Barium Sulfate and the later by Quddus [12] for the Calcium Sulfate on stainless steel. Also it is worth mentioning that, as the speed of rotation increased, the scale deposition on the metal surface got harder and stiffer and more compact with the increase in the weight gained on the metal surface. These results were more evident in titanium than in coated carbon steel.

4.2 Morphological Study of CaSO4 Scale

A solid titanium bar was cut into a 2.0 mm thick disc to study the scale morphology on titanium. The disc surfaces were polished and then cleaned by using acetone and distilled water to ensure that the samples' surface was free of contamination. The titanium disc is shown in Figure 4-23. After cleaning, the disc was fitted in a Teflon holder and then put at the bottom of the test rig. The experiment was run at 1000 RPM for 1.0, 2.0, 3.0 and 4.0 hours to study the Calcium Sulfate ($CaSO_4$) scale morphology.

Figure 4-23: Titanium Disc Sample

The Scanning Electron Microscopic (SEM) examination revealed various crystal structures comprising prismatic rods and needles-like growth. At some locations, plates-like growth was noticed. Generally the Calcium Sulfate ($CaSO_4$) crystals initially tended to grow perpendicular to the substrate surface and then to branch out randomly in all directions. This feature among others is perhaps a typical

characteristic of the Calcium Sulfate ($CaSO_4$) crystal growth mechanism. This feature was also observed earlier by Quddus [12] when he studied the Calcium Sulfate ($CaSO_4$) scale deposition on stainless steel metal surfaces.

The micrograph in Figure 4-24 shows the presence of a dense population of uniformly distributed Calcium Sulfate ($CaSO_4$) crystals on the entire surface of the substrate. Similar results were noticed by earlier studies for $BaSO_4$ [11] and $CaSO_4$ [12] scale formation on stainless steel surfaces.

The micrographs of Figure 4-25 and Figure 4-26 show the prismatic rods and needles successively emanating from the already deposited primary crystals. These micrographs also show the perpendicular growth of the Calcium Sulfate ($CaSO_4$), which appeared as a pertinent mechanistic feature of $CaSO_4$ scale formation.

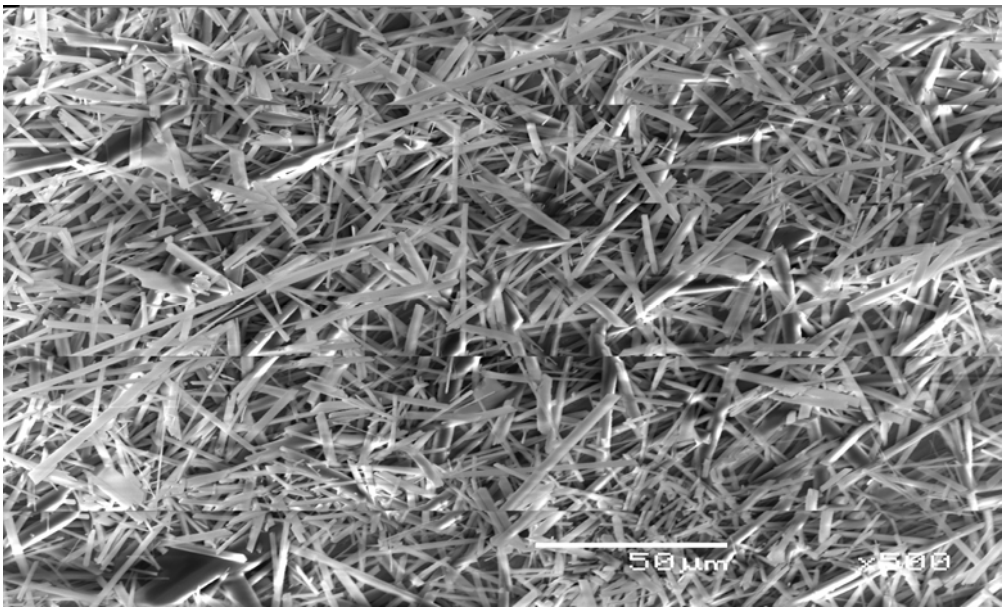

Figure 4-24: General Morphology of Calcium Sulfate (CaSO4) on Titanium Metal

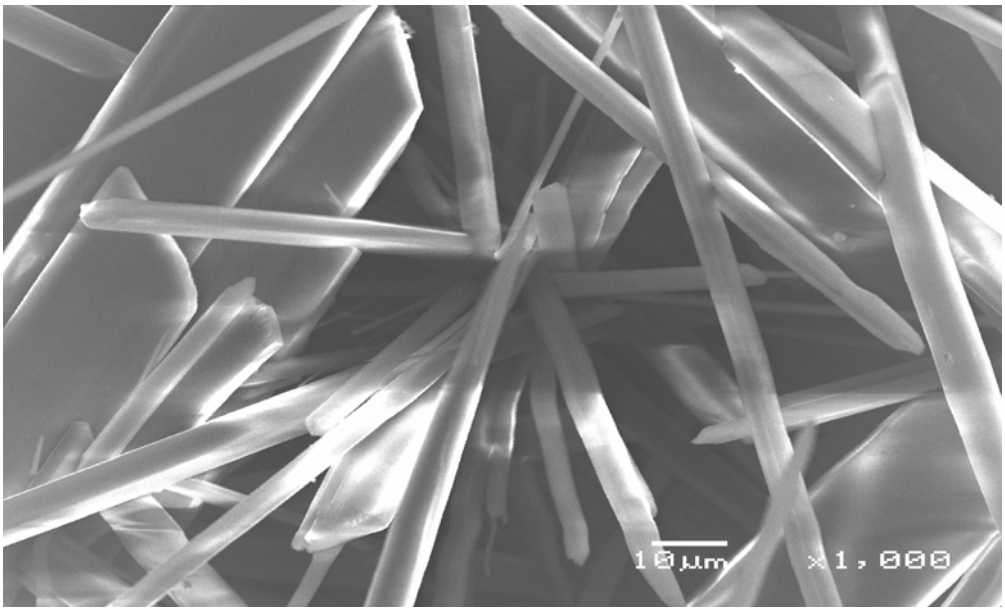

Figure 4-25: Prismatic Rods

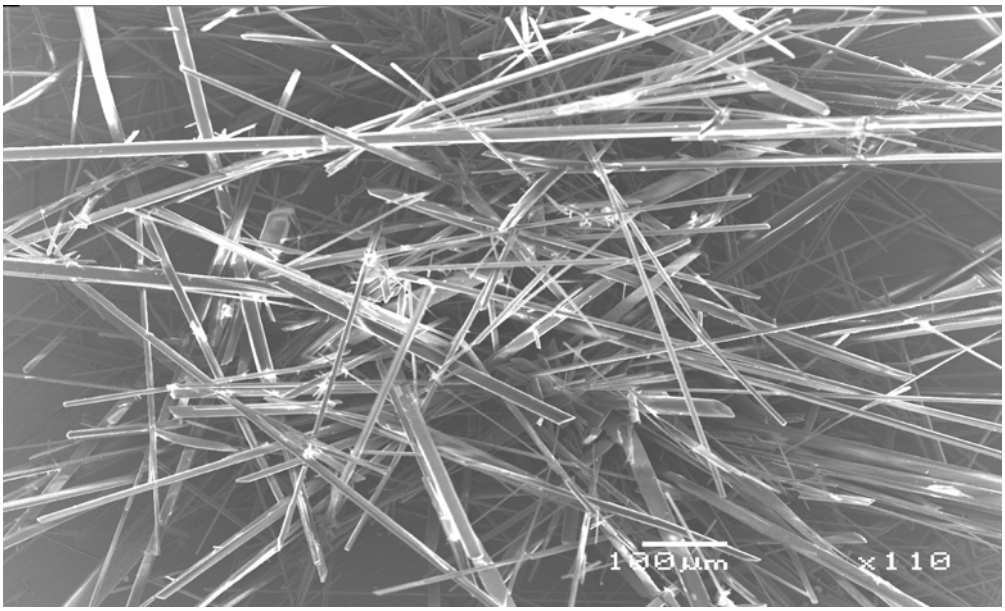

Figure 4-26: Needles Formation

It is envisaged that once a thin layer of scale is formed, the subsequent scale growth on it is much faster because of the readily available abundant nucleation sites as

compared to the initially polished surface. Another perception could be that the scaled surface becomes sufficiently rough with a larger surface area which promotes the deposition process more than does the bare surface.

CHAPTER 5

5.1 Economic Analysis

In this section, the economic analysis is presented to assess the benefits and advantages of applying coating on low-cost Carbon Steel as compared to the expensive Titanium metal tubing used in heat exchangers. Two important strategies for selecting materials without paying attention to other factors are as follows.

1. Minimum cost, which includes selection of low-cost materials followed by scheduled periodic replacements and corrosion control methods.

2. Minimum corrosion, which includes selection of the most corrosion-resistant material regardless of cost.

The common belief that advanced construction materials are expensive is not entirely true. Manufacturers often deliberately select low-cost materials for their products, because they believe that the manufacturing costs will be at a minimum and the product will therefore be competitively priced. Steels with improved properties often cost a little more per unit weight, but the total heat exchanger package is often less expensive. Savings are made possible because of the following factors.

1. Less material required

2. Less welding time and less filler material required

3. Shorter heat treatment cycles
4. Lower freight charges to destination
5. Easier handling requirements in the field during shipment and erection

Currently, the most common starting material is steel. About three-quarters of all heat exchangers are fabricated from carbon steel having 0.2 to 0.3 % carbon content to provide easy forming and welding. Although the strength-to-weight ratio of steel is not as favorable as those of certain titanium alloys when combined with cost, steel is often quite favorable. The factors that favor steel as a heat exchanger material are:

1. Steel is relatively inexpensive
2. Available in standard shapes
3. Well established mechanical properties
4. Fabricated by a wide variety of methods
5. Easily joinable by a wide variety of welding processes

To compare the cost of coated carbon steel tubes with titanium, the following equipment parameters will be assumed to ensure a fair comparison between both metals. An exchanger is made of 19.05 mm outside-diameter tubes, and it is 6.1 m long. The exchanger contains 1,000 tubes. Its pressure components are made from normal carbon steel.

The capital cost of an exchanger made of titanium tubes and carbon steel pressure components is approximately $ 400,000. The same exchanger made of carbon steel tubes costs $ 150,000 as the capital cost plus $ 30,000 for the internal coating. The net saving in the capital cost for an exchanger made of coated carbon steel tubes

compared to titanium tubes is $ 220,000. A typical cooling system plant contains at least four heat exchangers. So, if coated carbon steel is used for the tubing material in these heat exchangers, a cost saving of $ 880,000 would be achieved. This cost saving does not include the operation and production loss impact, since the coated carbon steel tubes mitigate fouling and they extend the operation period of the exchanger. So the operation span of the plant might be increased to four years instead of two years. Therefore, in addition to the capital cost saving, there is also an operation and maintenance cost saving which depends on each plant and process. Table 5-1 shows an economic comparison between two heat exchangers made of titanium and coated carbon steel.

Table 5-1: Economical Comparison Between Coated Carbon Steel and Titanium Heat Exchangers

	Material	Number of tubes	Capital cost (USD)	Coating cost (USD)	Total cost (USD)	Capital cost saving (%)
Exchanger 1	Carbon Steel	1000	150,000	30,000	180,000	45 % is the capital cost saving when using coated carbon steel in stead of titanium
Exchanger 2	Titanium	1000	400,000	0.0	400,000	

A heat exchanger is designed to have a twenty-year life. Titanium tubing material is usually replaced every ten years. The heat exchanger's tubing material is expected to be replaced twice during its operational life. In contrast, coated carbon steel tubes are

expected to run for a maximum of ten years before the coating loses its integrity, i.e. adhesion. Therefore, for both cases (coated carbon steel and titanium) the tubing material will be replaced twice during the heat exchanger's operational life. However, the coated carbon steel will result in greater cost benefits than the titanium during the same operational life.

CHAPTER 6

CONCLUSIONS AND RECOMMENDATIONS

6.1 Conclusions

Based on the results of the present experimental study, the following conclusions can be made:

1. It is concluded that 45.0 % of the equipment capital cost could be saved when using coated carbon steel instead of titanium.

2. Calcium Sulfate ($CaSO_4$) scale was reduced by 60 % when coated carbon steel samples were used instead of titanium.

3. Scale buildup on coated carbon steel and titanium surfaces is proportional to the rotational speed. This is clearer in the titanium samples. As the rotational speed increased, the deposition rate increased, which also was represented by more weight gained on the specimen surface. The scaling was less on coated carbon steel compared to the bare titanium surface.

4. At low speed, the deposited scale on both metals looked spongy, loose and less adherent to the metal surface. However, as the speed increased, the scale got more compact on the metal surface.

5. SEM examination indicated the scale morphology (structure) as prismatic rods and needles-like growth, and at some locations plate-like growth was also noticed. Generally the Calcium Sulfate ($CaSO_4$) crystals initially grew perpendicular to the metal surface, and then they branched out randomly.

6. The Calcium Sulfate ($CaSO_4$) crystal was distributed uniformly on the titanium surface. It was clearly seen that, once a thin layer of scale is formed, the subsequent scale layer growth on it is much faster, because of the readily available abundant nucleation sites as compared to the initially polished surface. The scaled surface becomes sufficiently rough, which promotes a faster deposition process than does the bare surface.

7. The data analysis of the Calcium Sulfate ($CaSO_4$) scale deposition rate showed that the rotational speed and the mixing of the solution had a strong influence on the rate of Calcium Sulfate deposition on coated carbon steel and titanium surfaces. The higher the speed of rotation, the more scale crystals adhered to the metal surface. The deposition rate increased linearly with the square root of the Reynolds number, which showed that the process is diffusion-controlled. It was noticed that, for both coated carbon steel and titanium, the deposition rate had a clear linear relationship with the speed of rotation.

8. Uncertainty analysis was conducted at three different Reynolds numbers (Re) for the measured variables such as specimen diameter (D), length (L), test duration (t) and weight gain (W_g) by the specimen. The selected Re were 1457, 14567 and 29135 which corresponded to low speed of rotation (100 RPM), medium speed (1000 RPM) and high speed (2000 RPM) respectively. Analysis results showed that, for both coated carbon steel and titanium samples, the percentage of uncertainty of the weight gain (W_g) was almost the same for all speeds of rotation as shown in Tables 3-1 to 3-6. However, the diameter (D) and length (L) had a low percentage of error. The percentage error of the test duration (t) was almost constant throughout the three different rotational speeds that were used for the uncertainty analysis.

6.2 Recommendations

The following are some recommendations for future studies and investigations:

1. The present experimental work can be extended to study different materials used in heat transfer equipment such as Copper, Copper-Nickel, Aluminum and different grades of Stainless Steel.

2. Further studies can be done to simulate the real situation by investigating the combined effects of different salts such as seawater.

3. The present work can be conducted and extended to other Reynolds numbers (Re).

4. The present study can be extended to investigate the effects of temperatures on the Calcium Sulfate ($CaSO_4$) scale deposition rate.

NOMENCLATURE

A_s	Surface area of the specimen (m^2)
D	Diameter of the specimen (m)
D_r	Deposition rate (g m^{-2} h^{-1})
L	Length of the specimen (m)
R_1	Radius of rotating specimen (m)
R_2	Radius of glass cell (m)
t	Duration of the experimental work (hr)
V	Tangential velocity (m/s)
W_g	Weight gained by the specimen (g)

Greek Symbols

ν	Kinematics viscosity of the solution (m^2 $.s^{-1}$)
ω	Angular velocity (rad/s)

REFERENCES

[1] Keith Gawlik, Stephen Kelley, Toshifumi Sugama, Ronald Webster and Walter Reams; “Development and Field Testing of Polymer-Based Heat Exchanger Coatings”, Proceeding World Geothermal Congress, pp. 3161-3165, 2000.

[2] R. Steinhagen, H. Muller-Steinhagen and K. Maani, “Problems and Costs Due to Heat Exchanger Fouling in New Zealand Industries”, Heat Transfer Engineering, Vol.14, no.1, pp. 19-30, 1992.

[3] Silverman D.C.; “Rotating Cylinder Electrode – Geometry Relationships for Prediction of Velocity – Sensitive Corrosion”, Corrosion, Vol. 44, pp.42-48, NACE, 1988.

[4] Gabe D. R., "The Rotating Cylinder Electrode", Journal of Applied Electrochemistry, Vol. 4, pp.91-108, 1974.

[5] H. M. Steinhagen; "Fouling of heat exchanger surfaces", Chemistry & Industry, Vol. 50, pp. 62-76, March 6, 1995.

[6] Neusen K. F., Chan S. H. and Zhou D. Z; "Heat transfer in Geophysical and Geothermal System", Vol. 76, pp. 45-50, ASME HTD, New York, 1987.

[7] Gudmundson J. S.; "Particulate Fouling", Fouling of Heat Transfer Equipment, Hemisphere Publishing Company, Washington D. C., pp. 357-387, 1981.

[8] Brian E. Hopkinson and Fermin S. Hernandez O.; “Use of Titanium in Petroleum Refining”, Material Performance, vol. 29, no. 9, pp. 48-52, Sep. 1990.

[9] K. Scholl, “Report on Liner Application/Heat Exchanger Construction Techniques”, National Renewable Energy Laboratory, NREL Milestone Report 2.2.3, July 1997.

[10] Neville A., Hodgkiess T. and Morizot A. P.; "Electrochemical assessment of calcium carbonate deposition using a rotating disc electrode (RDE)", Journal of Applied Electrochemistry, Vol. 29, pp. 455-462, 1999.

[11] Quddus A. and Allam I. M.; "$BaSO_4$ scale deposition on stainless steel" Desalination, Vol. 127, pp. 219-224, 2000.

[12] Quddus A. "Effect of hydrodynamics on the deposition of $CaSO_4$ on stainless steel" Desalination, Vol. 142, pp. 57-63, 2002.

[13] Neville A., Morizot A. P.;"Calcareous scales formed by cathodic protection –an assessment of characteristic and kinetics", Journal of Crystal Growth, Vol. 243, pp. 490-502, 2002.

[14] Morizot A. P., Neville A. and Taylor J. D. "An Assessment of the Formation of Electrodeposited Scales Using Scanning Electron and Atomic Microscopy", Journal of Crystal Growth, Vol. 23, pp. 2160-2165, 2002.

[15] Chen T., Neville A. and Yuan M.; "Calcium carbonate scale formation-assessing the initial stages of precipitation and deposition", Journal of Petroleum Science & Engineering, Vol. 46, pp. 185-194, 2005.

[16] D. R. Gabe, G. D. Wilcox, J. G. Garcia and F. C. Walsh " The Rotating Cylinder Electrode: its continued development and application", Journal of Applied Electrochemistry, Vol. 28, pp. 759-780, 1998.

[17] C. A. Branch and H. Muller-Steinhagen "Influence of Scaling on the Performance of Shell-and-Tube Heat Exchangers." Heat Transfer Engineering, Vol. 12, no. 2, pp.35-43, 1991.

[18] F. Fahiminia, A. Paul Watkinson and N. Epstin "Investigation of Initial Fouling Rates of Calcium Sulfate Solution Under Non-boiling Conditions." Engineering Conferences International Symposium Series, Vol. RPI, Article 5, 2003.

[19] R. Sheikhholeslami and M. Ng "Calcium Sulfate Precipitation in the Presence of Nondominant Calcium Carbonate: Thermodynamics and Kinetics." Ind. Eng. Chem. Res., Vol. 40, pp. 3570-3578, 2001.

[20] R. M. Behbahani, H. Muller-Steinhagen and M. Jamialahmadi "Investigation of Scale Formation in Heat Exchangers of Phosphoric Acis Evaporaters Plants." the Canadian Journal of Chemical Engineering, Vol. 84, pp. 82-103, April 2006.

[21] Helalizadeh, M. Steinhagen and M. Jamialahmadi "Crystallization Fouling of Mixed Salts During Convective Heat Transfer and Sub-Cooled Flow Boiling Conditions." Engineering Conferences International Symposium Series, Vol. RPI, Article 6, 2003.

[22] Q. Yang, Y. Liu, A. Gu, J. Ding, Z. Shen; "Investigation of Induction Period and Morphology of CaCO3 Fouling on Heated Surface" Chemical Engineering Science, Vol. 57, pp. 921-931, 2002.

[23] D. G. Klaren, E. F. Boer and D. W; "Zero Fouling Self Cleaning Heat Exchanger" Heat Transfer Engineering, vol. 28(3), pp. 216-221, 2007.

[24] Liu G., Tree D. A., and High M. S.; "Relationship Between Rotating Disc Corrosion Measurment and Corrosion in Pipe Flow" The Journal of Science and Engineering Corrosion, Vol. 50, pp. 584-596. NACE, 1994.

[25] Efrid K. D., Wright E. J., Boros J. A. and Hailey T. G.; The Journal of Science and Engineering Corrosion, Vol. 49, pp. 992-1007. NACE, 1993.

[26] Silverman D.C.; "Rotating Cylinder Electrode for Velocity Sensitivity Testing", Corrosion, Vol. 40, pp.220-227. NACE, 1984.

[27] Ashiru O. A. and Farr J. P.; "Kinetics of Reduction of Silver Complexes at a Rotation Disk Electrode (RDE)", Journal of Electrochemistry Society, Vol. 139, pp.2806-2818, 1992.

[28] Neville A., Morizot A. P Hodgkiess T.; "Electrochemical aspects of surface/solution interactions in scale initiation and growth", Material Performance, Vol. 50, pp. 203-211, May 1998.

[29] Coleman, H. W. and Steele, W. G.; "Experimental and Uncertainty Analysis for Engineers", Wiley, New York, 1999.

[30] Taylor B.N. and Kuyatt C. E.; "Guidelines for Evaluating and Expressing the Uncertainty of NIST Measurement Results", National Institute of Standards and Technology, 1994.

[31] Figliola R. S., and Beasely, D. E.; "Theory and Design of Mechanical measurements", 3rd Edition, Wiley Publishing house, 2000.

[32] V. G. Levich, "Physicochemical Hydrodynamics", Prentice-Hall, Englewood Cliffs, NJ, 1962.

Vita

- Dhawi A. Al-Otaibi
- Born in Khobar, Saudi Arabia, 09/09/1978
- Received Bachelor's degree in Mechanical Engineering from King Fahd University of Petroleum and Minerals (KFUPM), Dhahran, Saudi Arabia, in 2001 with First Honor.
- Currently working in Saudi Aramco with the Consulting Services Department as a Heat Exchangers Engineer.
- Completed Master's degree in Mechanical Engineering at KFUPM, 2008 with First Honor.

Appendix

This appendix is included here to show all the experimental results and data collection during the Thesis research. The purpose is to help other researchers to recognize the methodology and the experimental results, and thus to build their future experiments on these values.

Figures A-1 and A-3 show the best fitted straight lines for the Calcium Sulfate ($CaSO_4$) deposition rate on coated carbon steel for both linear and logarithmic values of deposition rate respectively. As shown by these figures, the lines are almost coincident. The deposition rate of Calcium Sulfate ($CaSO_4$) increases slightly with the Re on the coated carbon steel samples. The increase is insignificant. Therefore, the deposition rate profiles can be assumed to be constant as the Re increases.

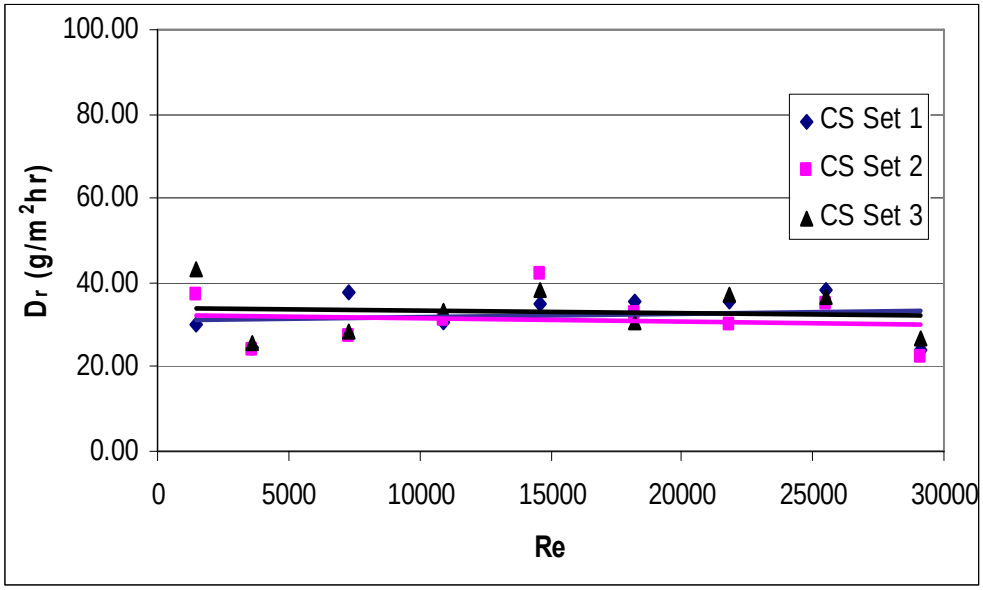

Figure A-1: Linear Best Fit in Deposition Rate on Coated Carbon Steel for Three Sets

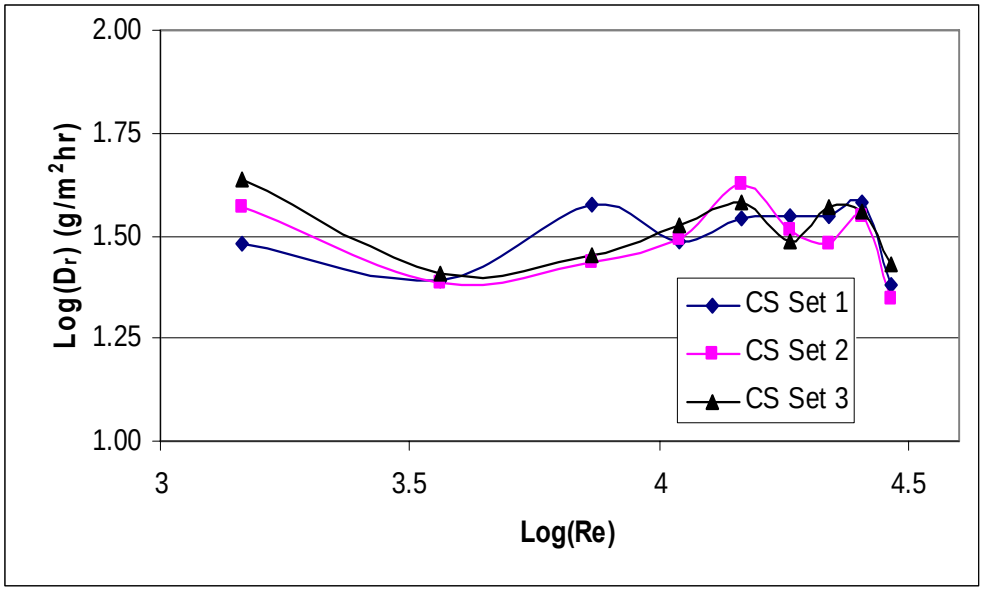

Figure A-2: Logarithmic Deposition Rate vs. Logarithmic Re on Coated Carbon Steel for Three Sets

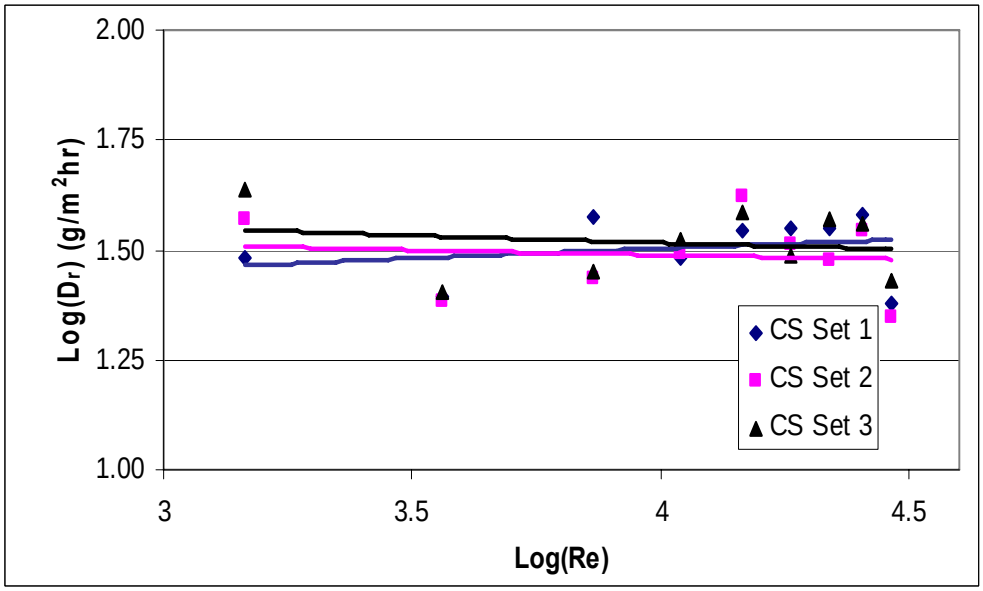

Figure A-3: Linear Best Fit in Logarithmic Deposition Rate vs. Logarithmic Re on Coated Carbon Steel for Three Sets

The following graphs are for the titanium samples. Each graph shows three repetitions to compare the deposition accumulation at the same Re (or rotational speed in RPM). These three tests are presented by Set 1, Set 2 and Set 3 respectively.

Figures A-4 and A-6 show the curves of the three experimental sets of the Calcium Sulfate ($CaSO_4$) deposition rate and the logarithmic values of the deposition rate respectively for the titanium specimens. Each test was repeated three times to verify and compare the deposition rate of Calcium Sulfate ($CaSO_4$) on these samples. As shown by these figures, the three curves are almost identical. Therefore, at the same Re, these three sets have almost the same deposition rate of Calcium Sulfate ($CaSO_4$). At certain values of the Re, the Calcium Sulfate ($CaSO_4$) deposition rate varies with +/- 8 % differences. These differences resulted from the experimental uncertainty.

Figures A-5 and A-7 show the curves of the three experimental sets for the best fitted straight lines for the Calcium Sulfate ($CaSO_4$) deposition rate and logarithmic values of the deposition rate respectively on titanium specimen. As shown by these figures, these lines are almost identical. The deposition rate of Calcium Sulfate ($CaSO_4$) increases as the Re increases on the titanium samples. The deposition rate increase is significant compared to the coated carbon steel samples.

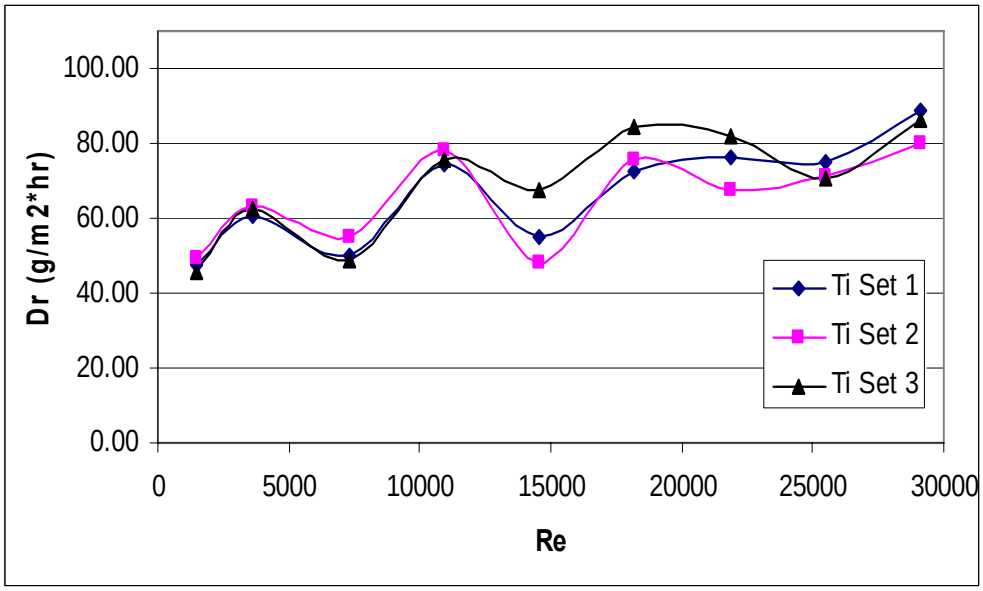

Figure A-4: Deposition Rate on Titanium for Three Sets

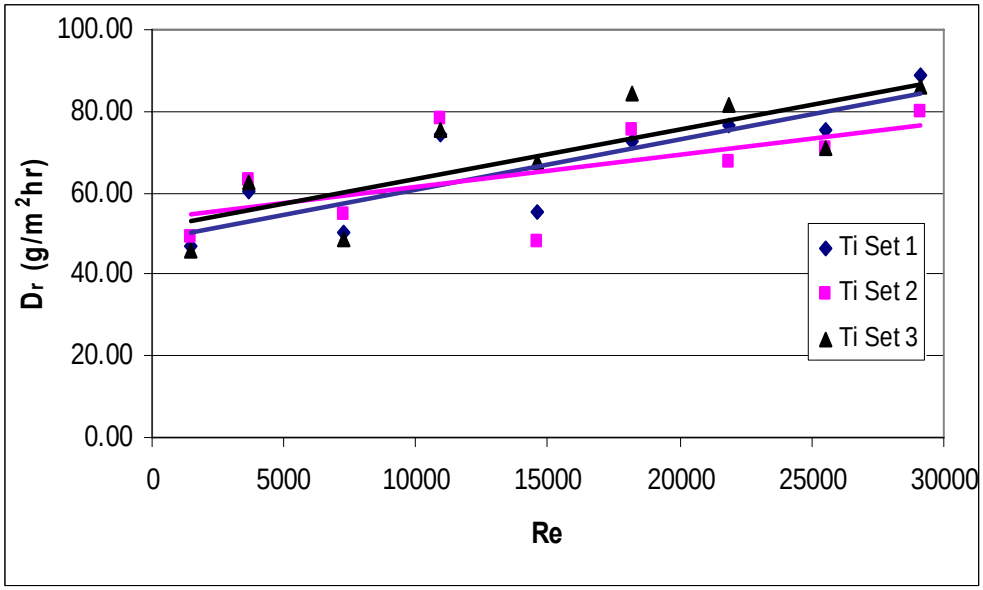

Figure A-5: Linear Best Fit in Deposition Rate on Titanium for Three Sets

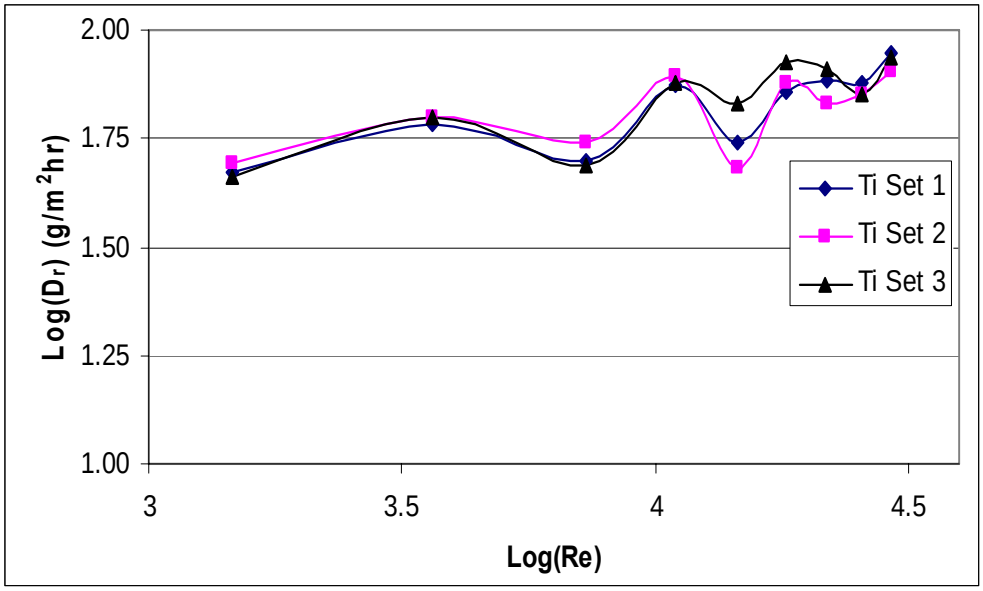

Figure A-6: Logarithmic Deposition Rate vs. Logarithmic Re on Titanium for Three Sets

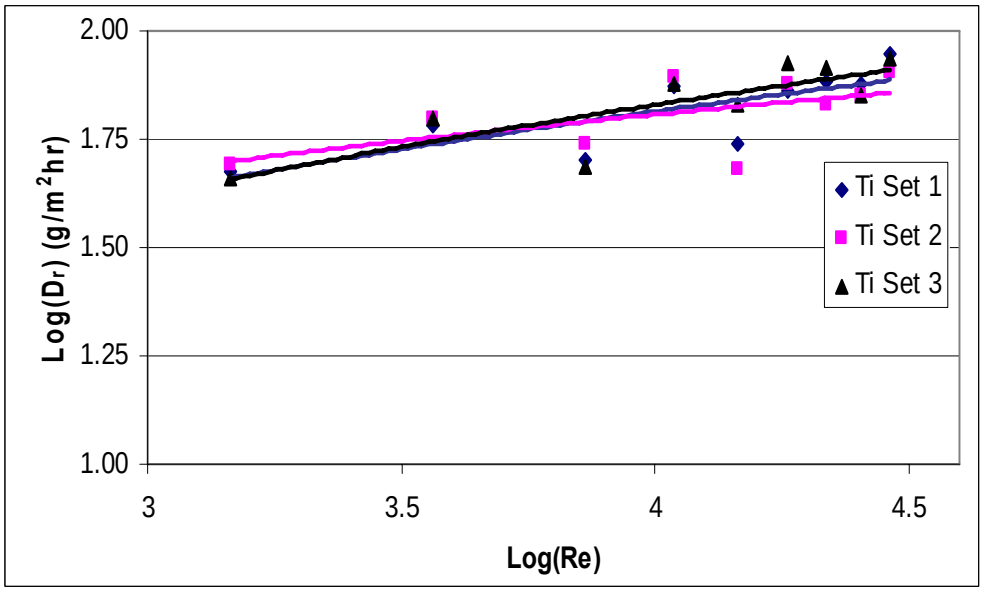

Figure A-7: Linear Best Fit in Logarithmic Deposition Rate vs. Logarithmic Re on Titanium for Three Sets

Figures A-8 and A-10 show the overall comparison of the deposition rate of the Calcium Sulfate ($CaSO_4$) scale and the logarithmic values of deposition rate respectively on both coated carbon steel and titanium samples. It is presented by six different curves. The Calcium Sulfate ($CaSO_4$) deposition rate increases more as the Re increases for the titanium samples as shown in these graphs. However, the deposition rate increases slightly for the coated carbon steel samples.

Figures A-9 and A-11 show the best fitted straight lines for the Calcium Sulfate ($CaSO_4$) deposition rate and logarithmic values of deposition rate respectively on both coated carbon steel and titanium samples. They support the results presented in Figures A-9 and A-11. Again, it is clear from these figures that the Calcium Sulfate ($CaSO_4$) deposition rate increases more as the Re increases for the titanium samples but it increases slightly for the coated carbon steel samples.

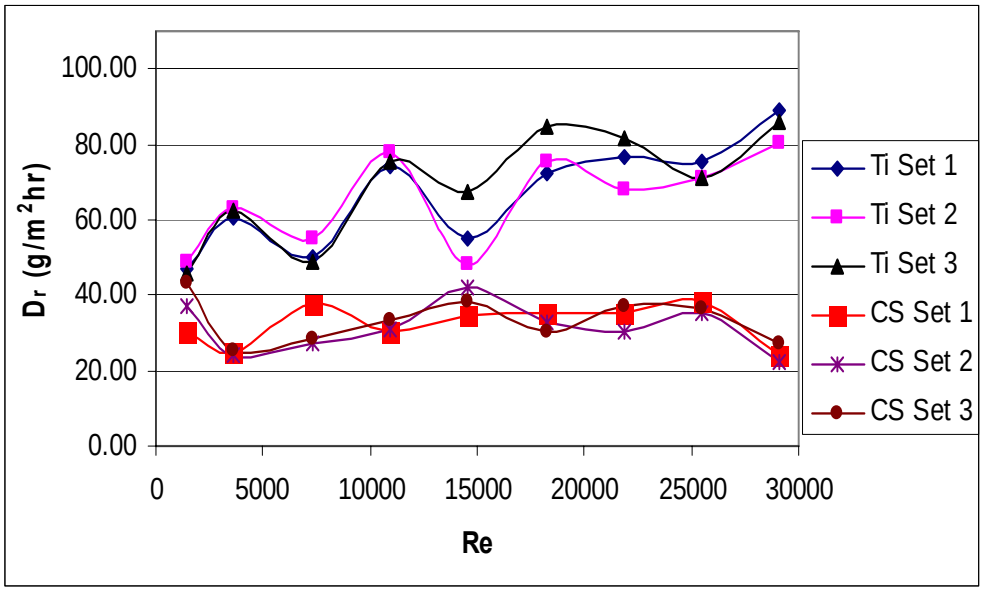

Figure A-8: Deposition Rate on Coated Carbon Steel and Titanium Metals

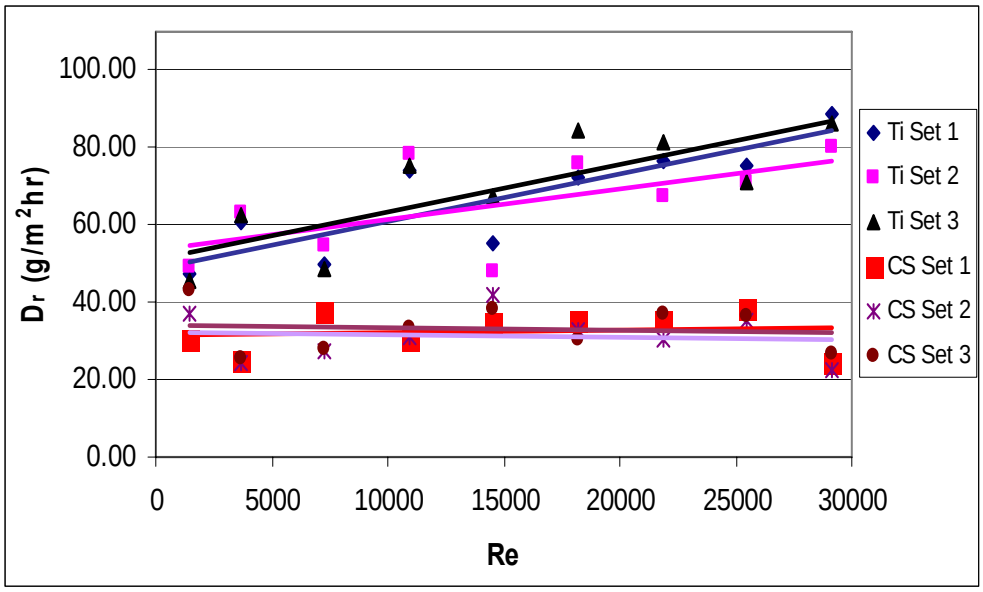

Figure A-9: Linear Best Fit in Deposition Rate on Coated Carbon Steel and Titanium Metals

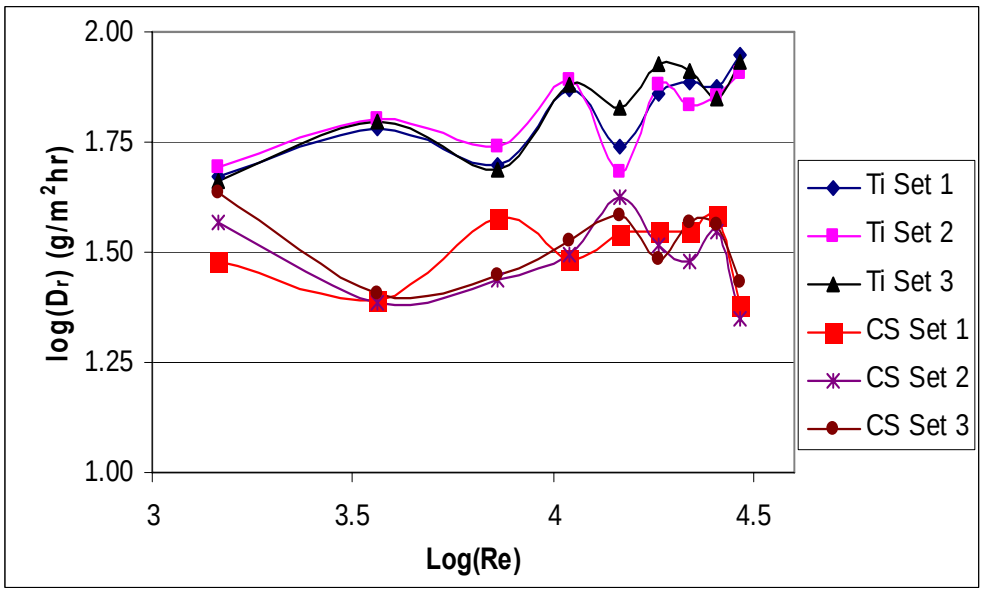

Figure A-10: Logarithmic Deposition Rate vs. Logarithmic Re for All Sets

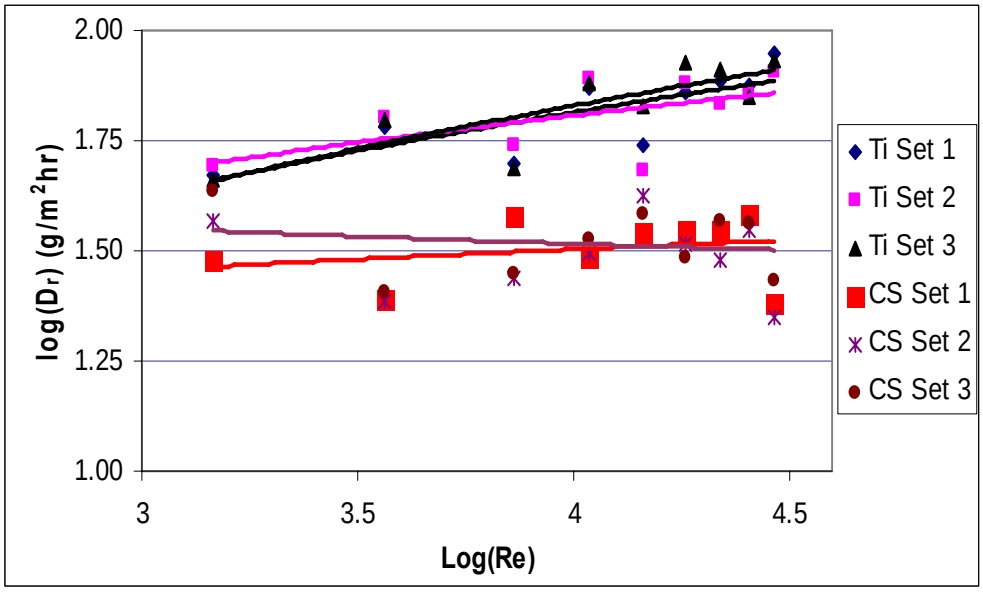

Figure A-11: Linear Best Fit in Logarithmic Deposition Rate vs. Logarithmic Re for All Sets

The average values of Calcium Sulfate ($CaSO_4$) deposition rate of the three sets were calculated for both the coated carbon steel and the titanium surfaces. The average deposition rate versus the Reynolds number (Re) is presented for both metal surfaces in the following paragraphs.

Figures A-12 and A-14 compare the average deposition rate of the Calcium Sulfate ($CaSO_4$) scale and the logarithmic values of deposition rate respectively on both the coated carbon steel and the titanium samples. The average of the three scale readings were taken at the same Re for each material. The Calcium Sulfate ($CaSO_4$) deposition rate increased more as the Re increased for the titanium samples. However, the deposition rate increased slightly for the coated carbon steel samples. These figures show that the deposition rate increases with the rotational speed on the titanium

surface, but its increase on the coated carbon steel samples is insignificant. So it can be stated that the deposition rate on coated carbon steel is constant, while it increases as the Re increases for the titanium.

Figures A-13 and A-15 show the best fitted straight lines for the average Calcium Sulfate ($CaSO_4$) scale and logarithm of the average Calcium Sulfate ($CaSO_4$) deposition rate respectively on both the coated carbon steel and the titanium metals versus the logarithm of Reynolds number (Re). The Calcium Sulfate ($CaSO_4$) deposition rate increases more as the Re increases for the titanium samples, but it increases slightly for the coated carbon steel samples. The results presented in these figures are in agreement with the results shown earlier in Figures A-12 and A-14.

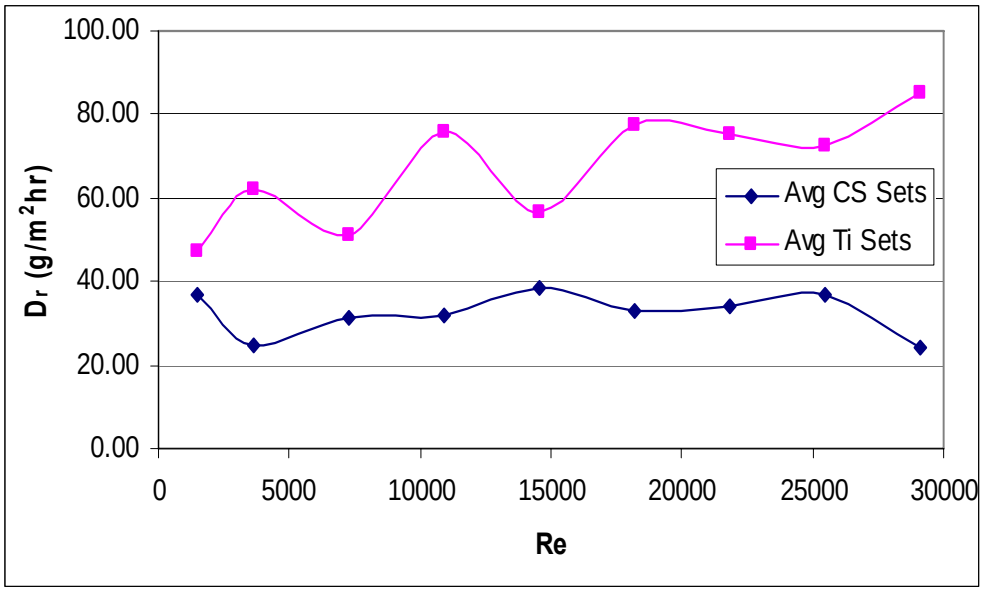

Figure A-12: Average Deposition Rate on Coated Carbon Steel and Titanium Metals

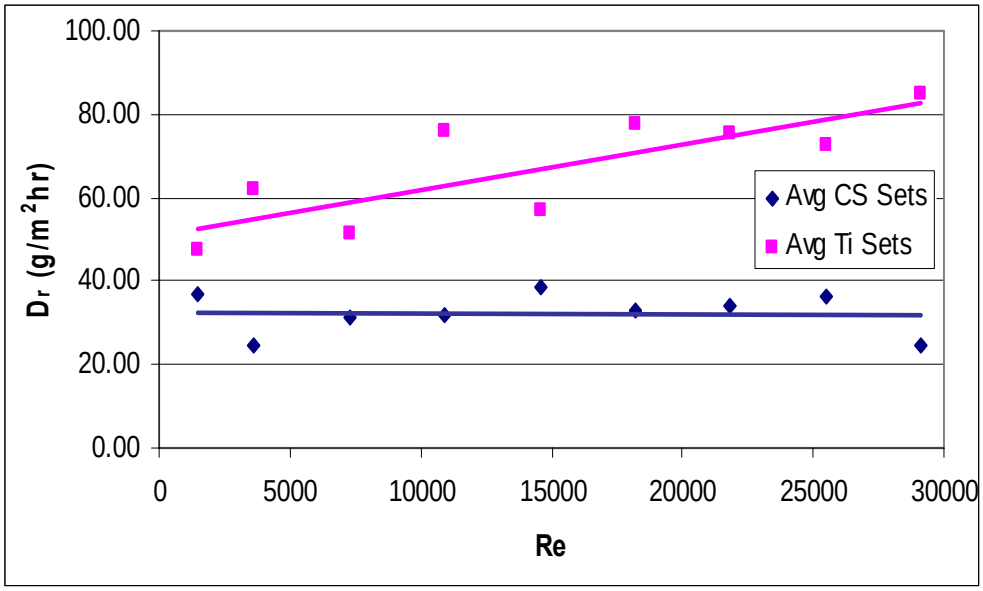

Figure A-13: Average Linear Best Fit in Deposition Rate on Coated Carbon Steel and Titanium Metals

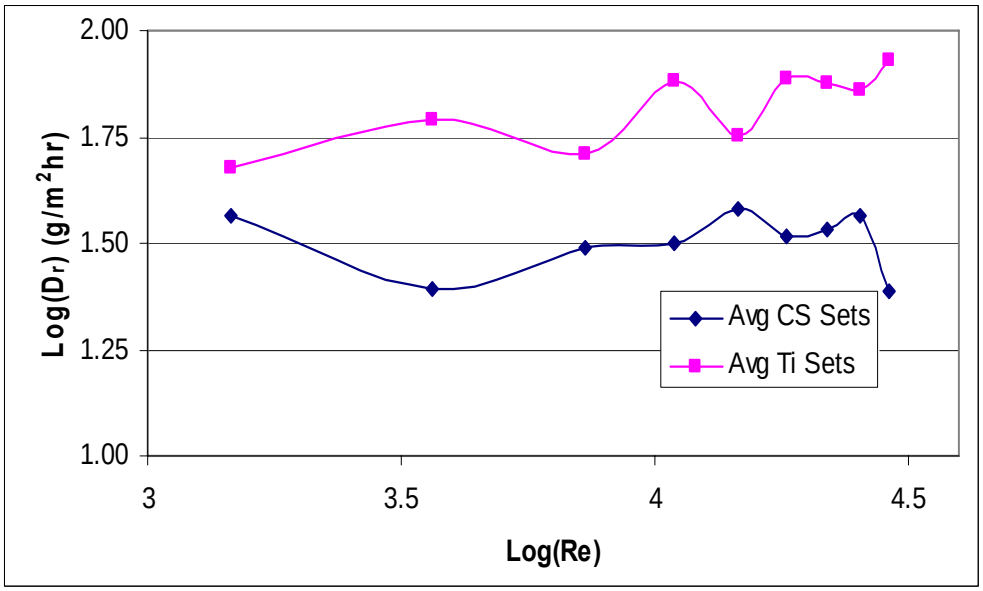

Figure A-14: Average Logarithm (Deposition Rate) vs. Logarithm (Re)

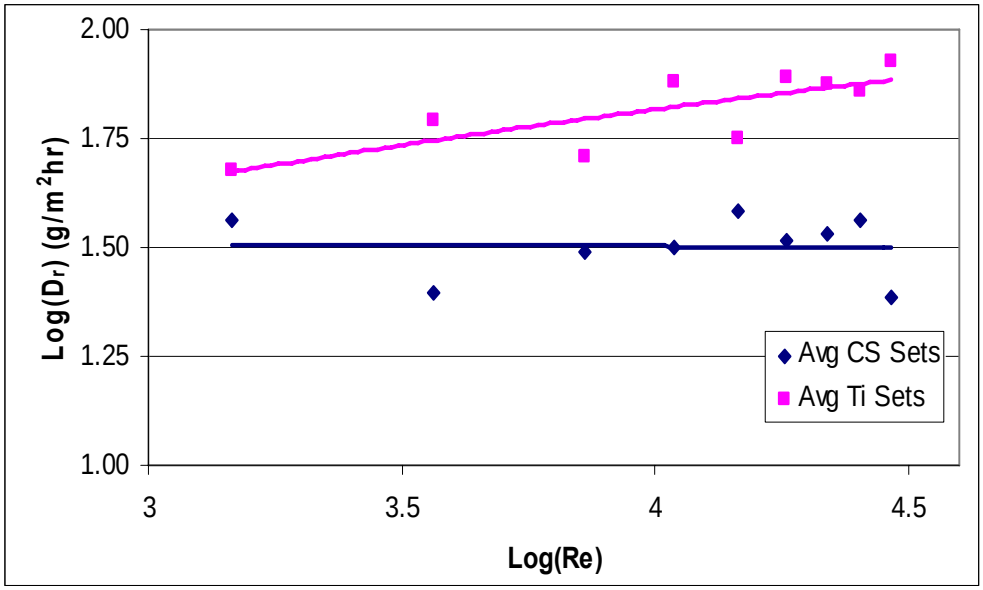

Figure A-15: Average Linear Best Fit in Logarithm (Deposition Rate) vs. Logarithm (Re)